

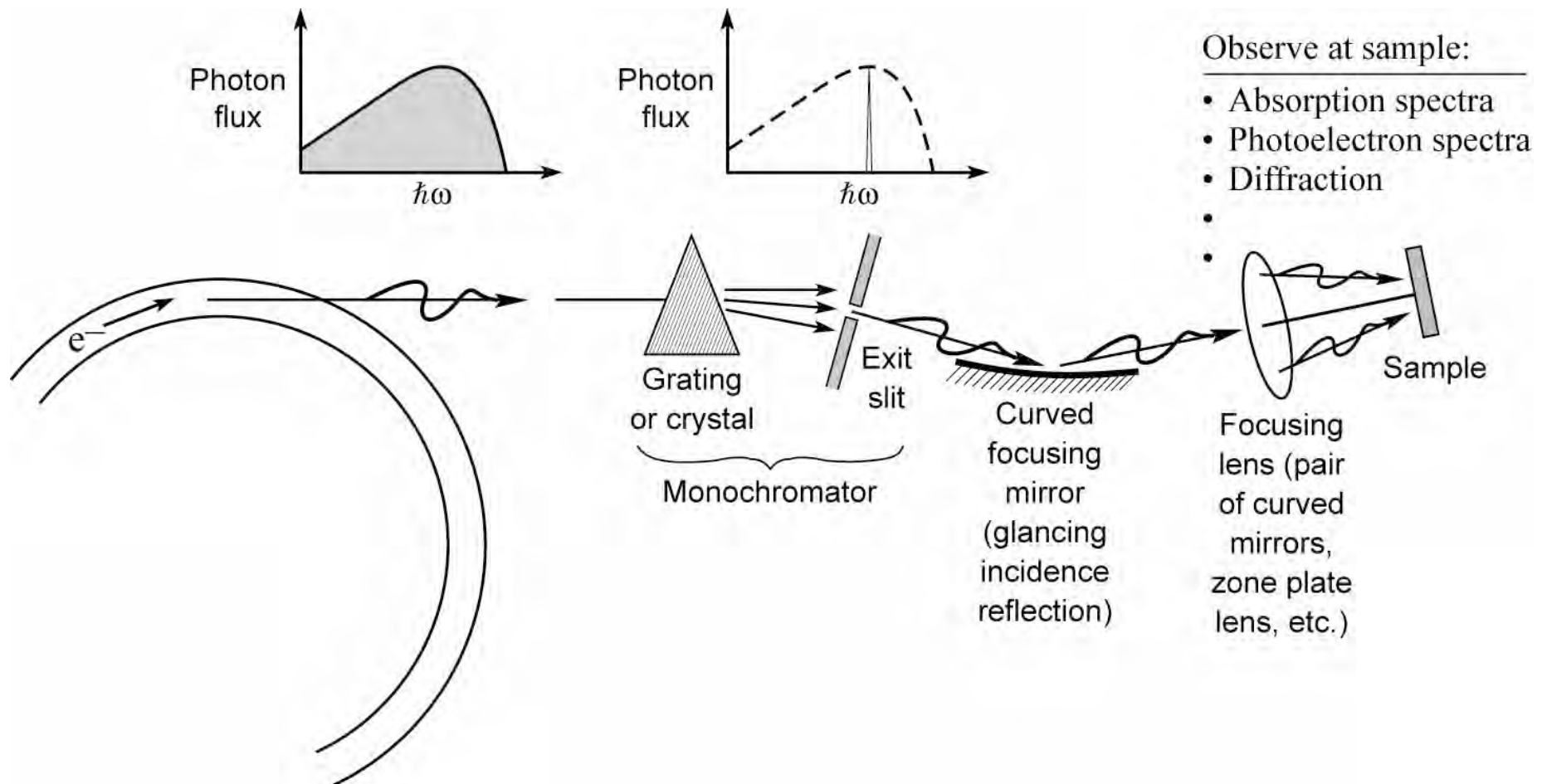


# **EUV and Soft X-Ray Beamlines**

David Attwood  
University of California, Berkeley  
and  
Advanced Light Source, LBNL

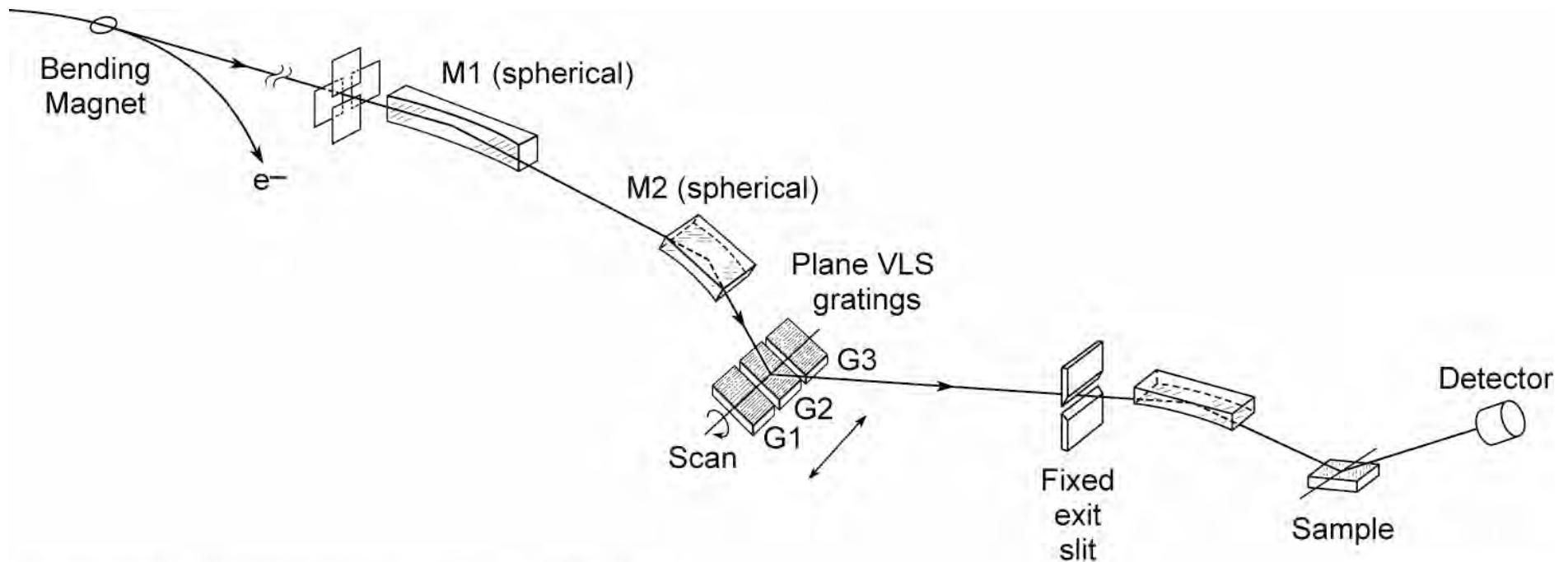
Cheiron School  
October 2010  
SPring-8

# Beamlines are used to transport photons to the sample, and take a desired spectral slice



Ch05\_F01b\_BLtransport.ai

# A typical beamline: monochromator plus focusing optics to deliver radiation to the sample



Courtesy of James Underwood (EUV Technology Inc.)

XBD9509-04496\_Jan04.ai

# Typical parameters for synchrotron radiation

Facility	ALS	New Subaru	APS	SP-8
Electron energy	1.90 GeV	1.00 GeV	7.00 GeV	8.00 GeV
$\gamma$	3720	1957	13,700	15,700
Current (mA)	400	100	100	100
Circumference (m)	197	119	1100	1440
RF frequency (MHz)	500	500	352	509
Pulse duration (FWHM) (ps)	35-70	26	100	120
<i>Bending Magnet Radiation:</i>				
Bending magnet field (T)	1.27	1.03	0.599	0.679
Critical photon energy (keV)	3.05	0.685	19.5	28.9
Critical photon wavelength	0.407 nm	1.81 nm	0.636 Å	0.429 Å
Bending magnet sources	24	4	35	23
<i>Undulator Radiation:</i>				
Number of straight sections	12	4	40	48
Undulator period (typical) (cm)	5.00	5.40	3.30	3.20
Number of periods	89	200	72	140
Photon energy ( $K = 1, n = 1$ )	457 eV	117 eV	9.40 keV	12.7 keV
Photon wavelength ( $K = 1, n = 1$ )	2.71 nm	10.6 nm	1.32 Å	0.979 Å
Tuning range ( $n = 1$ )	230-620 eV	43-170 eV	3.5-12 keV	4.7-19 keV
Tuning range ( $n = 3$ )	690-1800 eV	130-500 eV	10-38 keV	16-51 keV
Central cone half-angle ( $K = 1$ )	35 $\mu$ rad	44 $\mu$ rad	11 $\mu$ rad	6.6 $\mu$ rad
Power in central cone ( $K = 1, n = 1$ ) (W)	2.3	0.15	12	16
Flux in central cone (photons/s)	$3.1 \times 10^{16}$	$7.9 \times 10^{15}$	$7.9 \times 10^{15}$	$7.9 \times 10^{15}$
$\sigma_x, \sigma_y$ ( $\mu$ m)	260, 16	450, 220	320, 50	380, 6.8
$\sigma'_x, \sigma'_y$ ( $\mu$ rad)	23, 3.9	89, 18	23, 7	16, 1.8
Brightness ( $K = 1, n = 1$ ) <sup>a</sup>				
[(photons/s)/mm <sup>2</sup> · mrad <sup>2</sup> · (0.1%BW)]	$2.3 \times 10^{19}$	$1.7 \times 10^{17}$	$5.9 \times 10^{18}$	$1.8 \times 10^{20}$
Total power ( $K = 1$ , all $n$ , all $\theta$ ) (W)	83	27	350	2,000
Other undulator periods (cm)	3.65, 8.00, 10.0	7.60	2.70, 5.50, 12.8	2.4, 10.0, 3.7, 12.0
<i>Wiggler Radiation:</i>				
Wiggler period (typical) (cm)	16.0		8.5	12.0
Number of periods	19		28	37
Magnetic field (maximum) (T)	2.1		1.0	1.0
$K$ (maximum)	32		7.9	11
Critical photon energy (keV)	5.1		33	43
Critical photon wavelength	0.24 nm		0.38 Å	0.29 Å
Total power (max. $K$ ) (kW)	13		7.4	18

<sup>a</sup>Using Eq. (5.65). See comments following Eq. (5.64) for the case where  $\sigma'_{x,y} = \theta_{\text{cen}}$ .

# Undulator radiated power in the central cone

$$\lambda_x = \frac{\lambda_u}{2\gamma^2} \left(1 + \frac{K^2}{2} + \gamma^2 \theta^2\right)$$

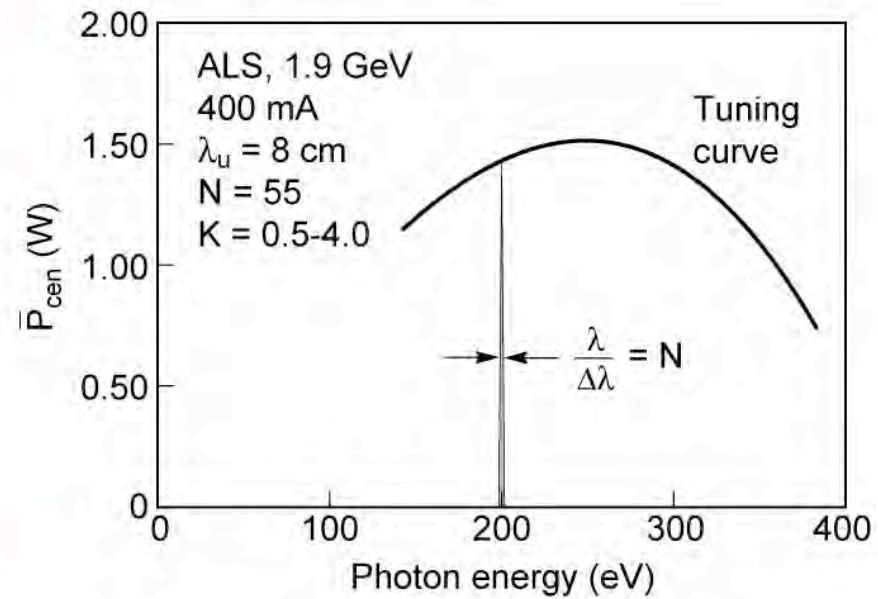
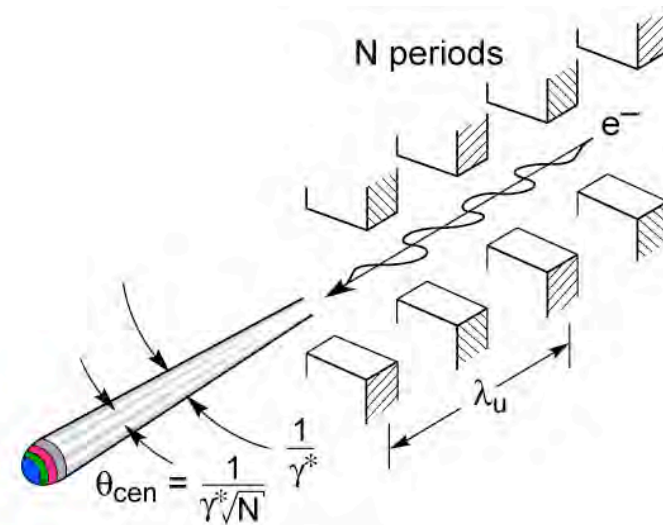
$$\bar{P}_{\text{cen}} = \frac{\pi e \gamma^2 I}{\epsilon_0 \lambda_u} \frac{K^2}{\left(1 + \frac{K^2}{2}\right)^2} f(K)$$

$$\theta_{\text{cen}} = \frac{1}{\gamma^* \sqrt{N}}$$

$$\left(\frac{\Delta\lambda}{\lambda}\right)_{\text{cen}} = \frac{1}{N}$$

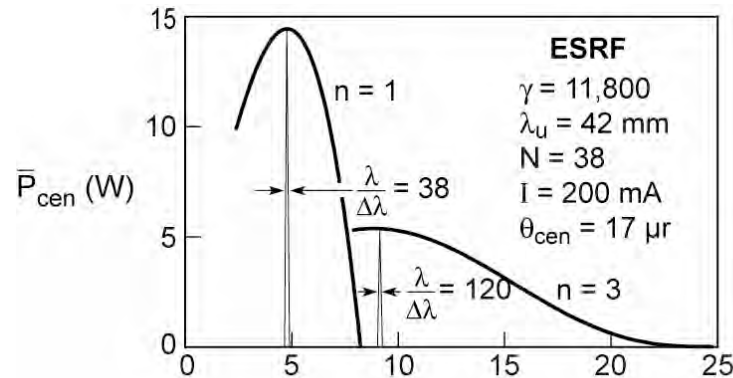
$$K = \frac{eB_0 \lambda_u}{2\pi m_0 c}$$

$$\gamma^* = \gamma / \sqrt{1 + \frac{K^2}{2}}$$





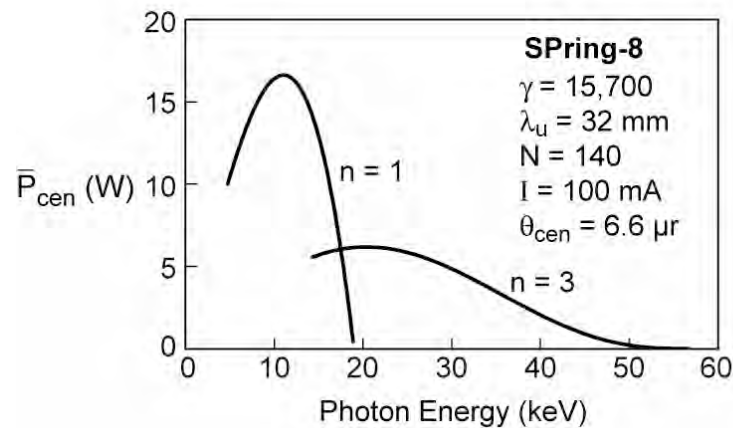
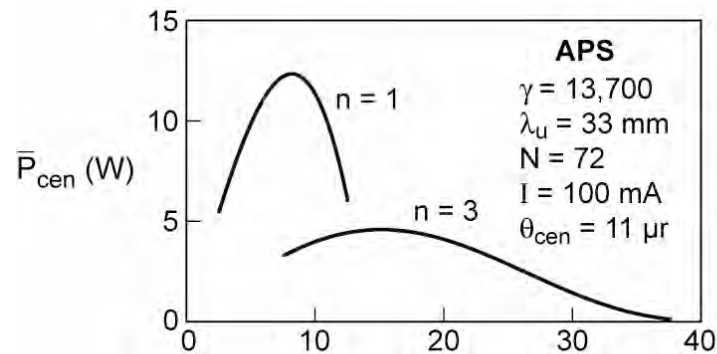
# Power in the central radiation cone for three x-ray undulators



$$\theta_{\text{cen}} = \frac{1}{\gamma^* \sqrt{N}}$$

$$\left[ \frac{\Delta\lambda}{\lambda} \right]_1 = \frac{1}{N}$$

$$\left[ \frac{\Delta\lambda}{\lambda} \right]_3 = \frac{1}{3N}$$



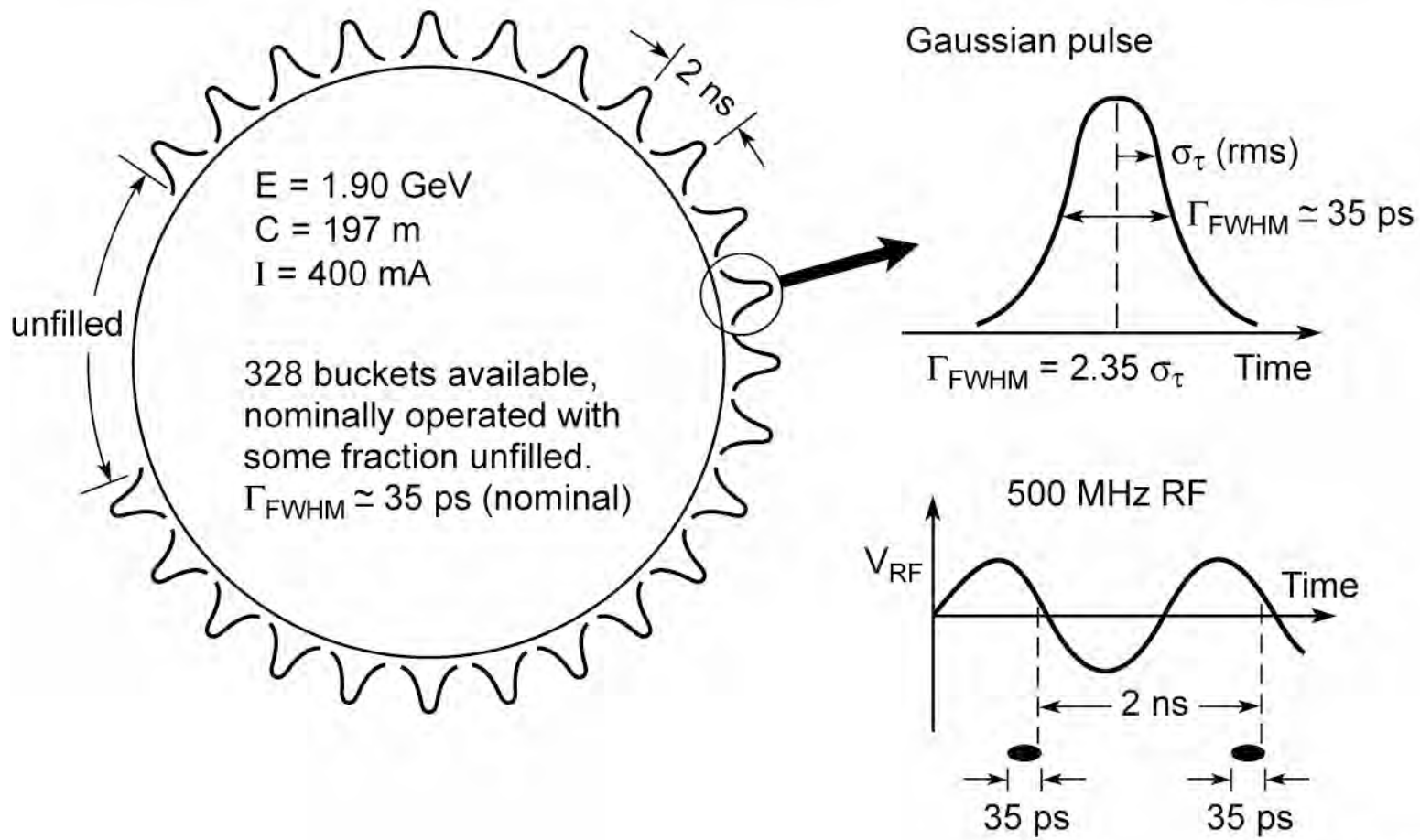
# Typical parameters for synchrotron radiation

Facility	ALS	New Subaru	APS	SP-8
Electron energy	1.90 GeV	1.00 GeV	7.00 GeV	8.00 GeV
$\gamma$	3720	1957	13,700	15,700
Current (mA)	400	100	100	100
Circumference (m)	197	119	1100	1440
RF frequency (MHz)	500	500	352	509
Pulse duration (FWHM) (ps)	35-70	26	100	120
<i>Bending Magnet Radiation:</i>				
Bending magnet field (T)	1.27	1.03	0.599	0.679
Critical photon energy (keV)	3.05	0.685	19.5	28.9
Critical photon wavelength	0.407 nm	1.81 nm	0.636 Å	0.429 Å
Bending magnet sources	24	4	35	23
<i>Undulator Radiation:</i>				
Number of straight sections	12	4	40	48
Undulator period (typical) (cm)	5.00	5.40	3.30	3.20
Number of periods	89	200	72	140
Photon energy ( $K = 1, n = 1$ )	457 eV	117 eV	9.40 keV	12.7 keV
Photon wavelength ( $K = 1, n = 1$ )	2.71 nm	10.6 nm	1.32 Å	0.979 Å
Tuning range ( $n = 1$ )	230-620 eV	43-170 eV	3.5-12 keV	4.7-19 keV
Tuning range ( $n = 3$ )	690-1800 eV	130-500 eV	10-38 keV	16-51 keV
Central cone half-angle ( $K = 1$ )	35 $\mu$ rad	44 $\mu$ rad	11 $\mu$ rad	6.6 $\mu$ rad
Power in central cone ( $K = 1, n = 1$ ) (W)	2.3	0.15	12	16
Flux in central cone (photons/s)	$3.1 \times 10^{16}$	$7.9 \times 10^{15}$	$7.9 \times 10^{15}$	$7.9 \times 10^{15}$
$\sigma_x, \sigma_y$ ( $\mu$ m)	260, 16	450, 220	320, 50	380, 6.8
$\sigma'_x, \sigma'_y$ ( $\mu$ rad)	23, 3.9	89, 18	23, 7	16, 1.8
Brightness ( $K = 1, n = 1$ ) <sup>a</sup>				
[(photons/s)/mm <sup>2</sup> · mrad <sup>2</sup> · (0.1%BW)]	$2.3 \times 10^{19}$	$1.7 \times 10^{17}$	$5.9 \times 10^{18}$	$1.8 \times 10^{20}$
Total power ( $K = 1$ , all $n$ , all $\theta$ ) (W)	83	27	350	2,000
Other undulator periods (cm)	3.65, 8.00, 10.0	7.60	2.70, 5.50, 12.8	2.4, 10.0, 3.7, 12.0
<i>Wiggler Radiation:</i>				
Wiggler period (typical) (cm)	16.0		8.5	12.0
Number of periods	19		28	37
Magnetic field (maximum) (T)	2.1		1.0	1.0
$K$ (maximum)	32		7.9	11
Critical photon energy (keV)	5.1		33	43
Critical photon wavelength	0.24 nm		0.38 Å	0.29 Å
Total power (max. $K$ ) (kW)	13		7.4	18

<sup>a</sup>Using Eq. (5.65). See comments following Eq. (5.64) for the case where  $\sigma'_{x,y} = \theta_{cen}$ .

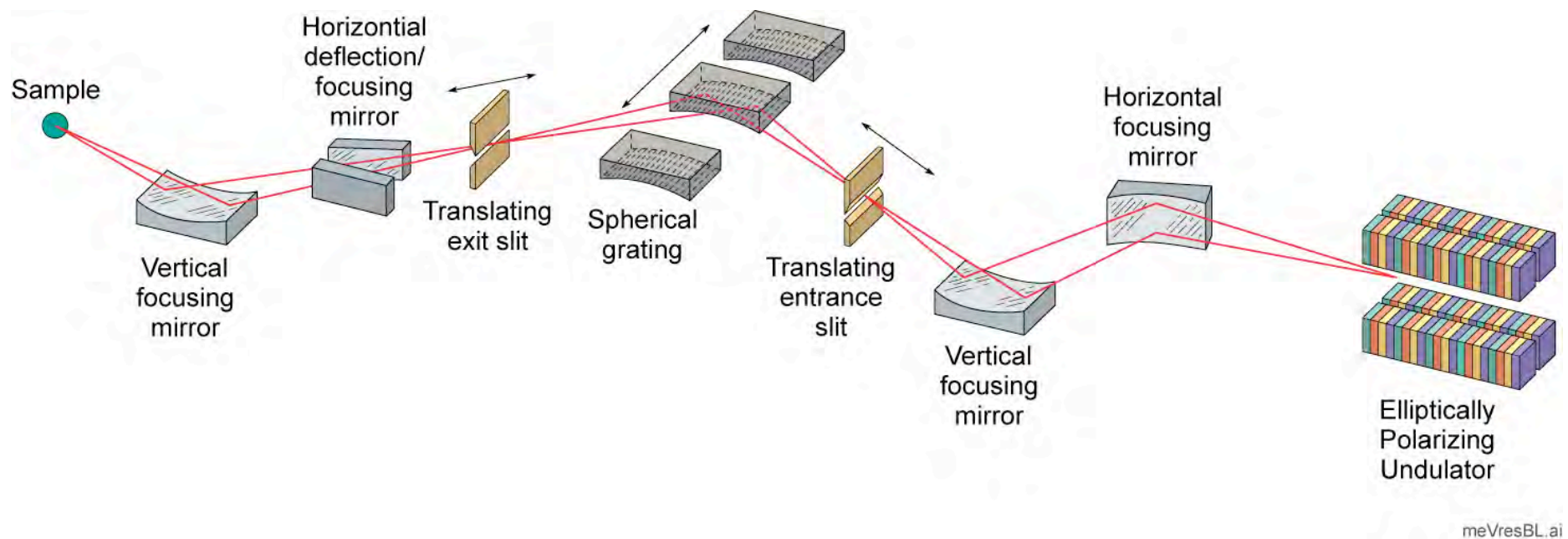
# Time structure of synchrotron radiation

The axial electric field within the RF cavity, used to replenish lost (radiated) energy, forms a potential well “bucket” system that forces electrons into axial electron “bunches”. This leads to a time structure in the emitted radiation.





## High spectral resolution (meV beamline)





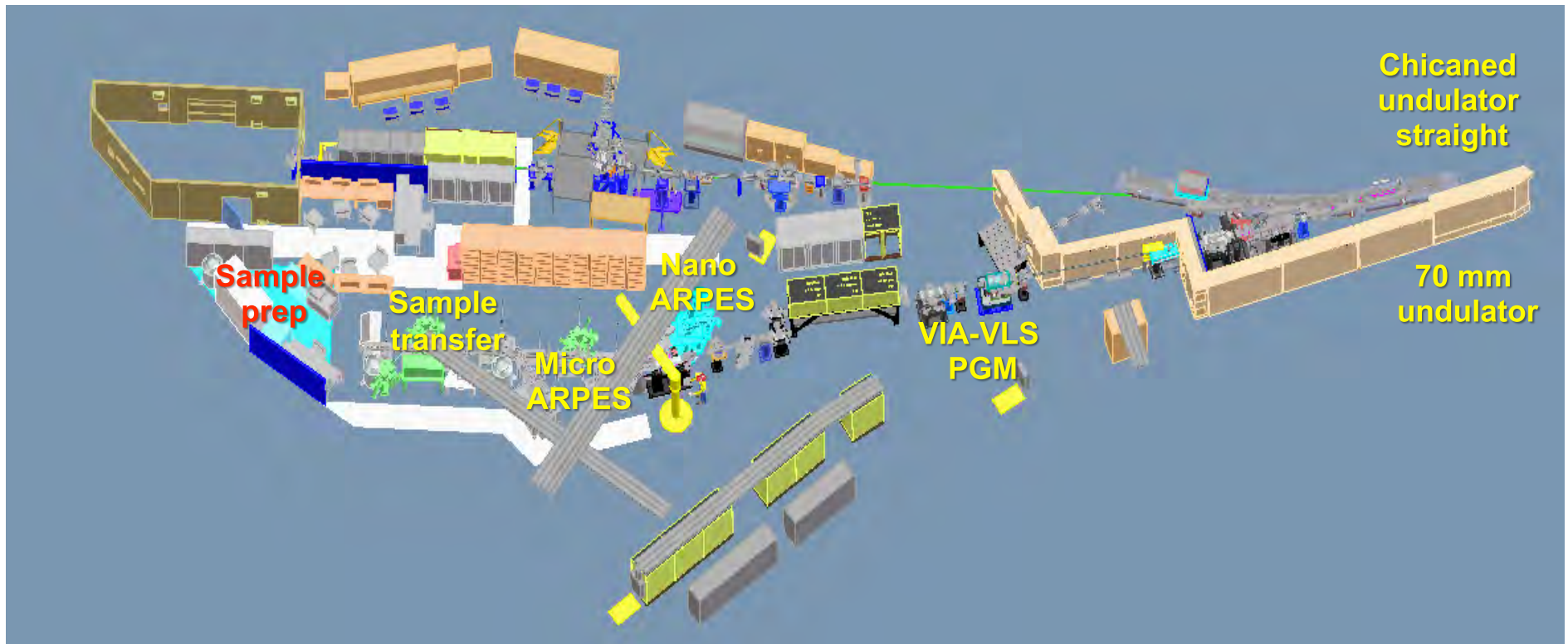
## Beamline 7.0 at Berkeley's Advanced Light Source





## MAESTRO: A new varied-line-space grating monochromator beam line for angle-resolved-photo-electron-spectroscopy with high spectral and spatial resolution at the Advanced Light Source

Jason Wells, Derek Yegian, Ken Chow, Eli Rotenberg, Aaron Bostwick, Geoff Gaines and Tony Warwick



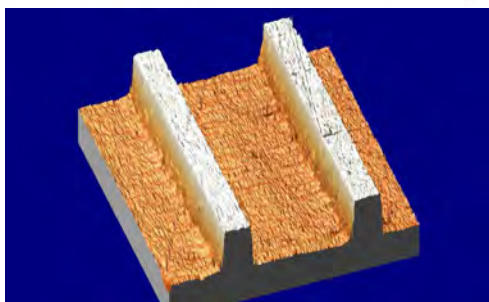
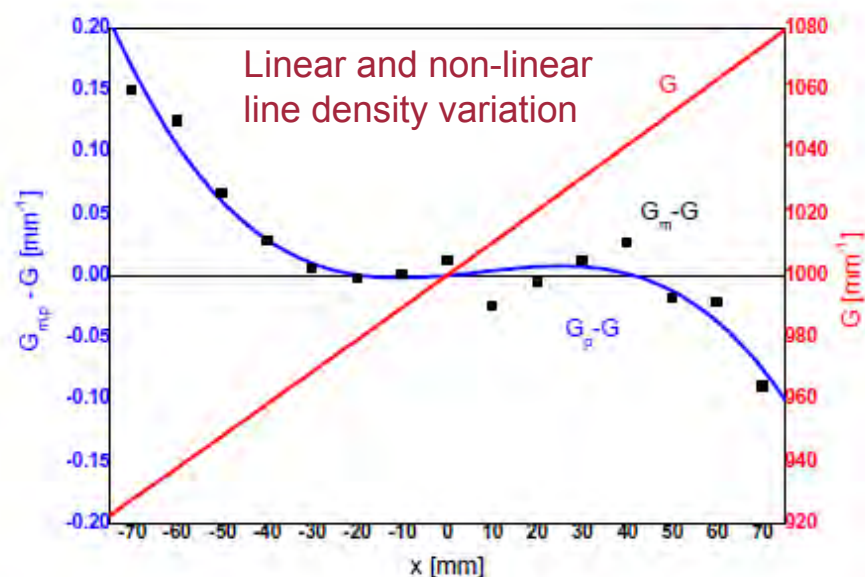
The latest soft x-ray undulator spectroscopy beam line planned for the ALS serves **MAESTRO** a new high resolution Angle Resolved Photo Emission facility with zone-plate focused nano-ARPES. The beam line design offers spectral resolution 1:30000 from 60eV to 400eV with an extended energy range from 20eV to 1000eV. Challenges include optical figure quality, thermal engineering, source size and stability and vibrations in the monochromator. The optical design is radical in that a VLS grating will provide all of the focusing in the dispersion direction, and the mirrors are plane, except for a sphere to collect and focus horizontally.

Courtesy of Eli Rotenberg and Tony Warwick (ALS)



# Varied line space gratings

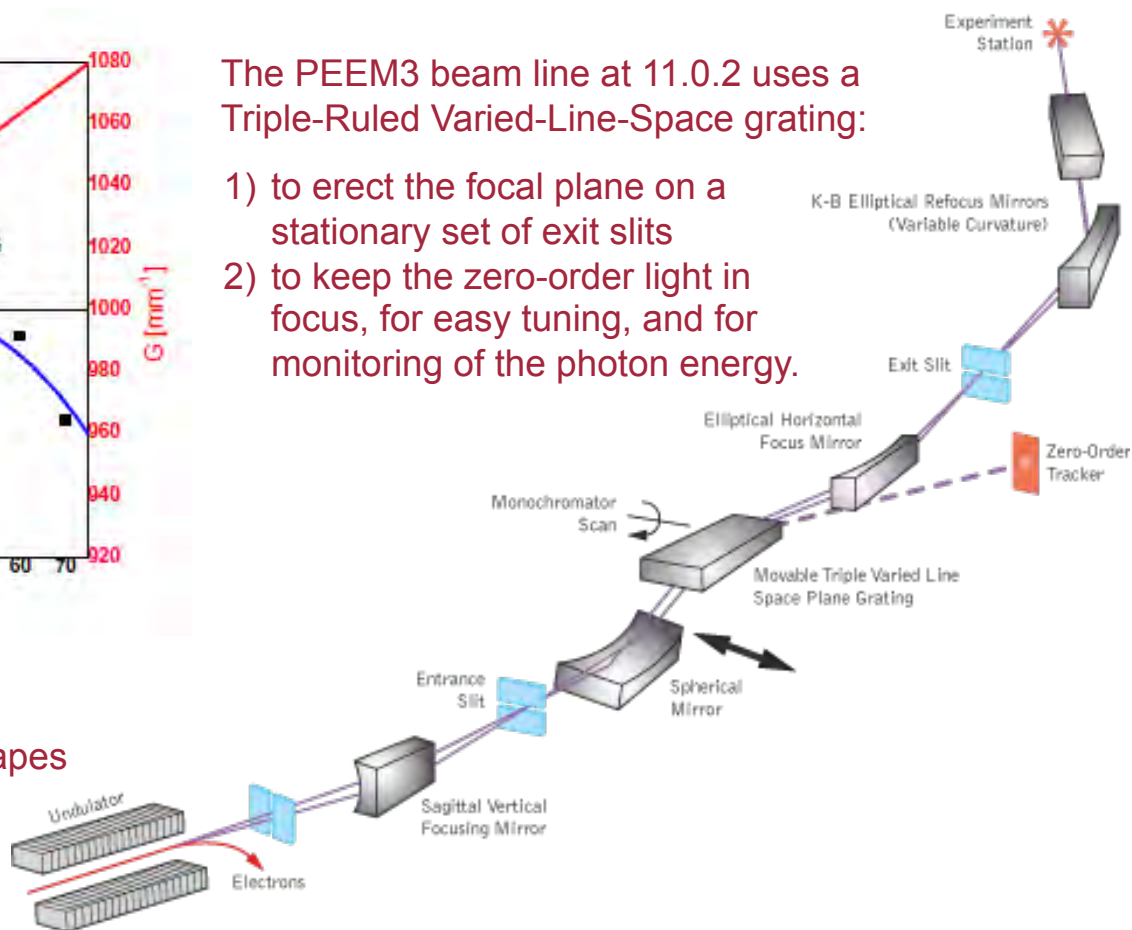
Varied-Line-Space Plane Gratings provide focusing and aberration correction along with the dispersion that they generate in the monochromator. They can be used to erect the monochromator focal plane, making the position of the focus at the exit slit (almost) stationary as the grating rotates to select the photon energy. Beyond that, they are now being used to replace the focusing from shaped optics, making beam lines cheaper and easier to align.



AFM  
measured  
groove shapes

The PEEM3 beam line at 11.0.2 uses a Triple-Ruled Varied-Line-Space grating:

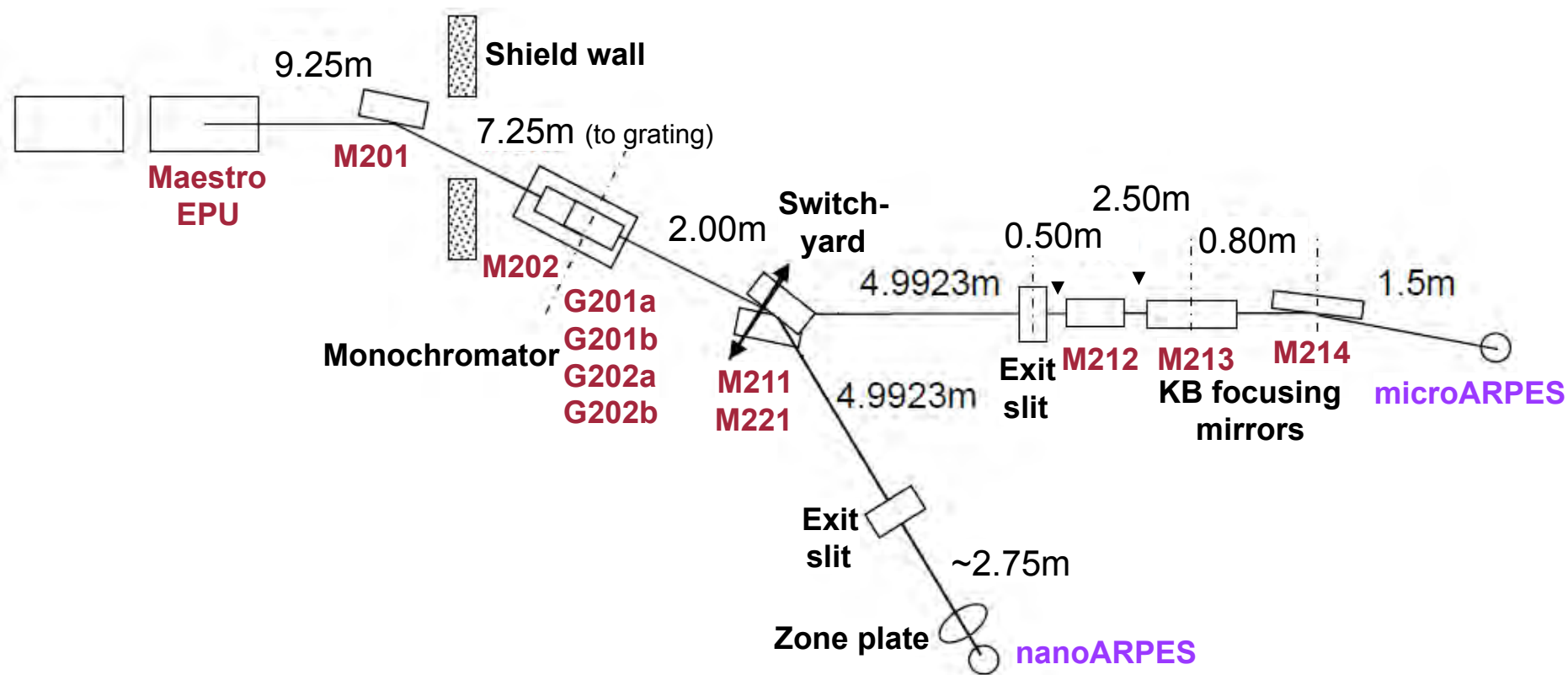
- 1) to erect the focal plane on a stationary set of exit slits
- 2) to keep the zero-order light in focus, for easy tuning, and for monitoring of the photon energy.



Courtesy of Tony Warwick (ALS)



# MAESTRO: A new varied-line-space grating monochromator beam line at the ALS

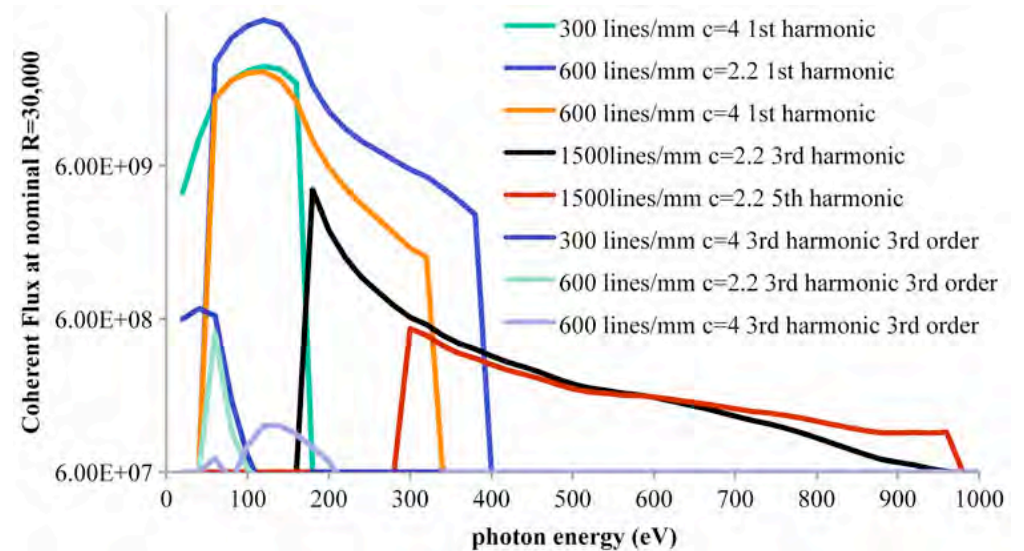
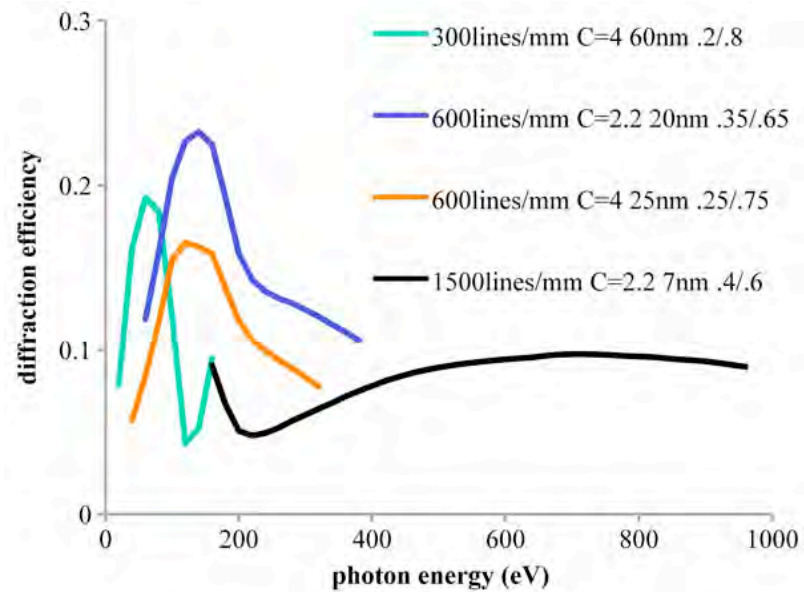


Courtesy of Tony Warwick (ALS)



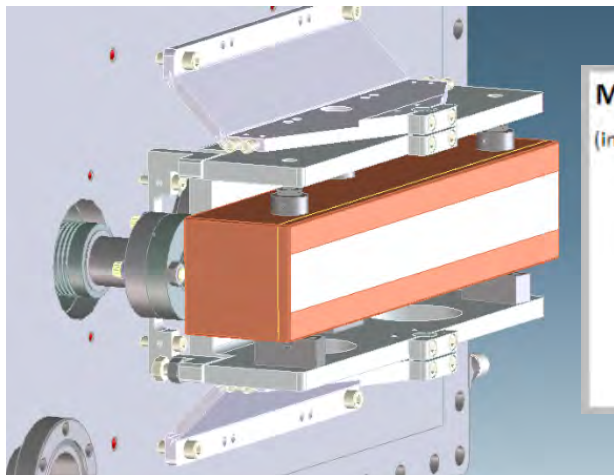


# MAESTRO at the ALS: gratings and efficiencies

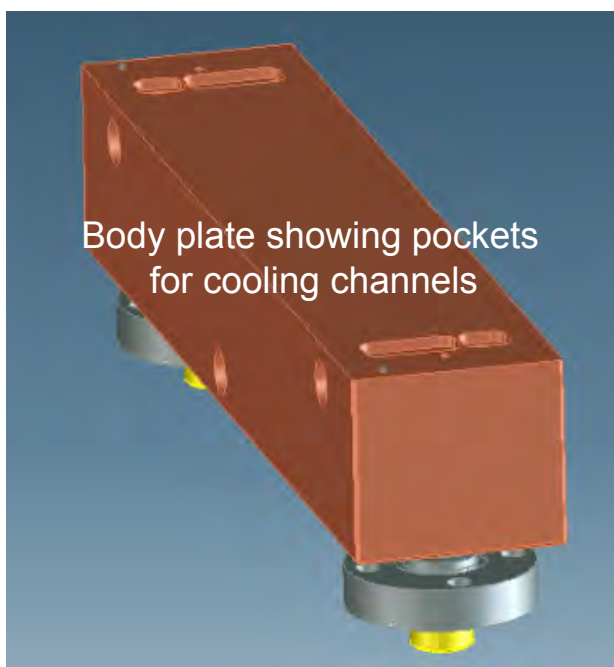


Courtesy of Tony Warwick (ALS)

# Water-cooled optics are essential: correcting slope errors due to a thermal bump



M201 Plane - Slope Errors ( $\mu\text{Rad}$ ) (internally cooled Glidcop, $10\text{K W/m}^2\text{K}$ )	<u>over full mirror substrate</u>		<u>over clear aperture</u>	
	60eV	20eV	60eV	20eV
Maximum Tangential Slope Error	28.2	61.3	28.2	61.3
Average Tangential Slope Error	2.4	4.9	3.0	6.1
RMS Tangential Slope Error	3.3	7.0	4.4	9.3
Maximum Sagittal Slope Error	36.4	75.1	36.4	75.1
Average Sagittal Slope Error	7.3	15.3	13.9	29.2
RMS Sagittal Slope Error	12.2	25.6	18.0	38.0



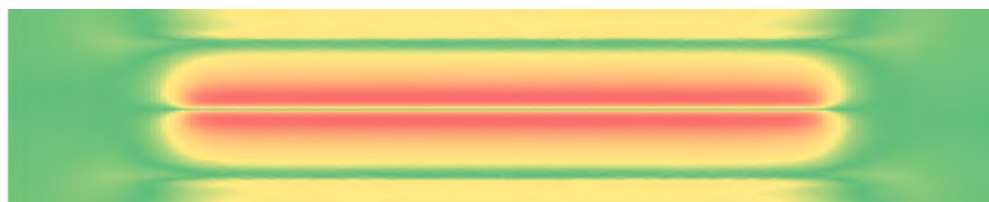
Height error



Tangential slope error



Sagittal slope error

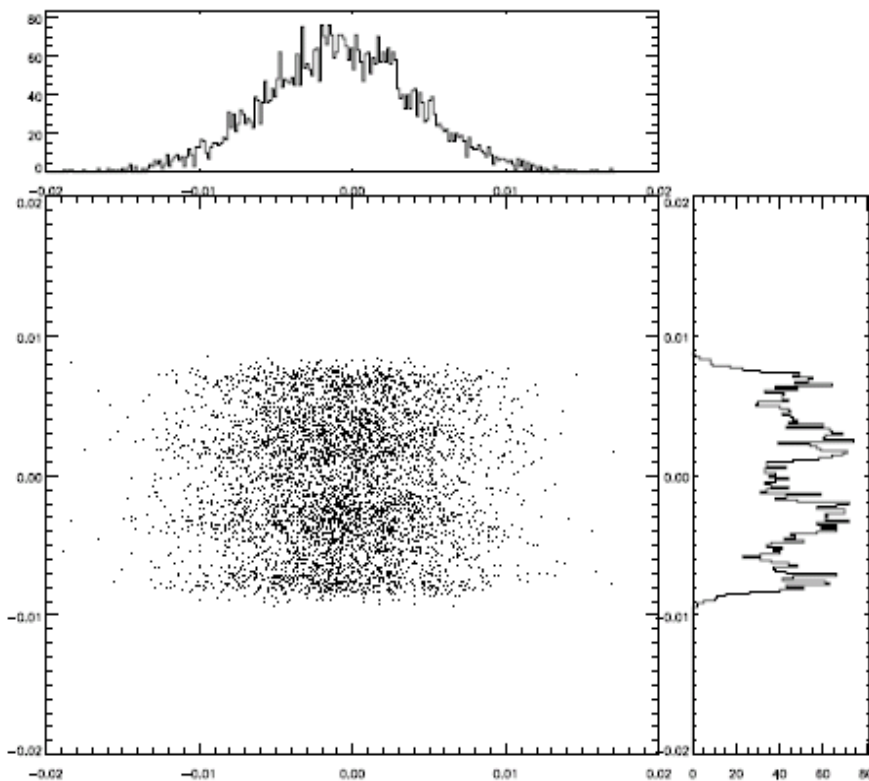


Courtesy of Tony Warwick (ALS)

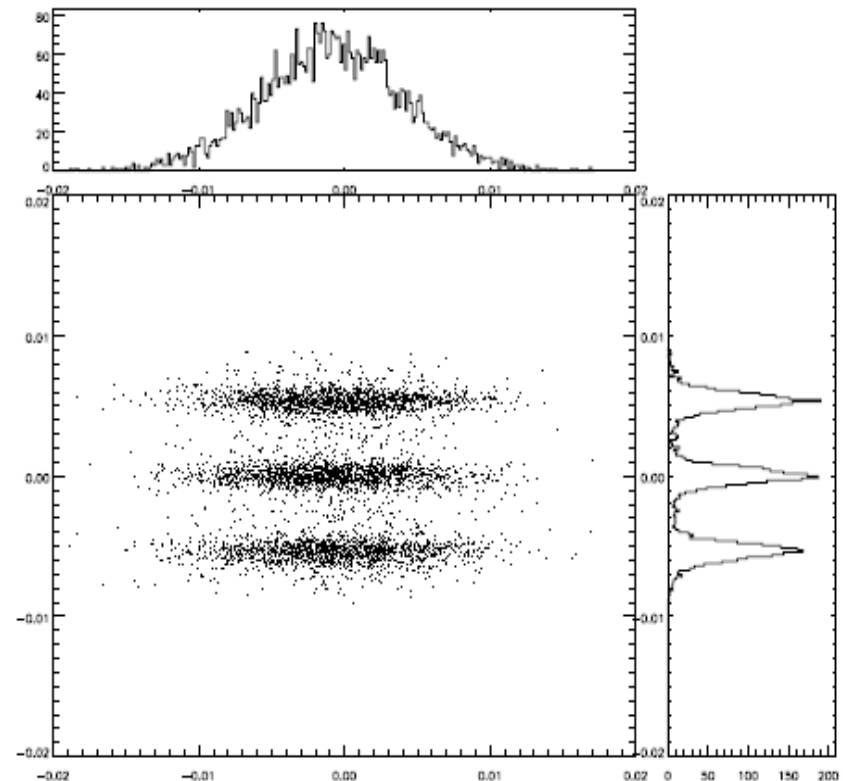


## Ray tracing beamlines is an important tool

Significant degradation of the spectral resolution occurs due to localized heating of M202. It is almost entirely corrected by adjusting the monochromator focusing parameter from 3.93 to 4.02. The engineering design will allow this mirror to be built with 1mm thick hot-wall and the actual thermal deformation is expected to be less.



600lines\_60eV\_10000\_c=3.93034\_18.7\_0.038\_  
1.5mmheatbump



600lines\_60eV\_10000\_c=4.02\_18.7\_0.038\_  
1.5mmheatbumpcorrected

Courtesy of Tony Warwick (ALS)



## References

Reininger, R., Kriesel, K., Hulbert, S.L., Sanchez-Hanke, C. and Arena, D.A., Rev. Sci. Instrum., 79, 033108 2008

Peterson, H., Jung, C., Hellwig, C. Peatman, W.B. and Gudat, W., Rev. Sci. Instrum. 66 (1995) 1

Follath, R., and Senf, F., Nucl. Instrum. Methods Phys. Res. A390 (1997) 388

Amemiya, K., Kitajima, Y., Ohta, T., and Ito, K., J. Synchrotron Radiation 3 (1996) 282

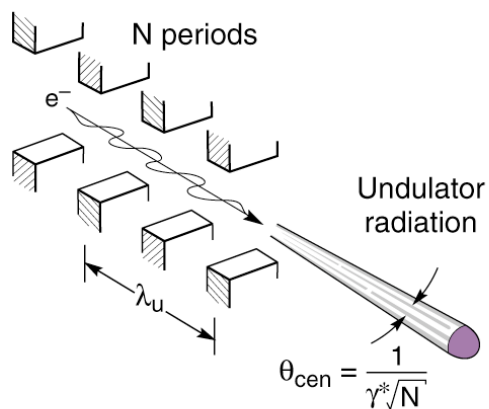
The original SHADOW package is available at [www.nanotech.wisc.edu/CNTLABS/shadow.html](http://www.nanotech.wisc.edu/CNTLABS/shadow.html) and with an IDL user interface at [www.esrf.fr/computing/scientific/xop](http://www.esrf.fr/computing/scientific/xop)

Undulator Radiation, Ellaume, P., in Undulators, Wigglers and their Applications, Onuki, H. and Ellaume, P. eds., Taylor and Francis.

Characteristics of Synchrotron Radiation, Kim, K., J., in Xray Data Booklet LBNL internal report (1986) PUB 490 [xdb.lbl.gov/xdb.pdf](http://xdb.lbl.gov/xdb.pdf)

D Fluckiger - Grating Solver Development Company Dec 2006 [www.gsolver.com](http://www.gsolver.com)

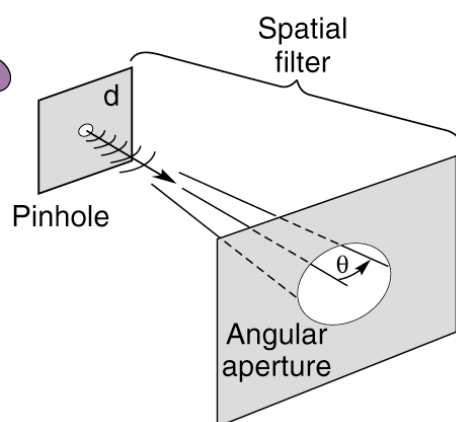
# Beamlines for spatially coherent undulator radiation



$\lambda = 11.2 \text{ nm}$



$\lambda = 13.4 \text{ nm}$



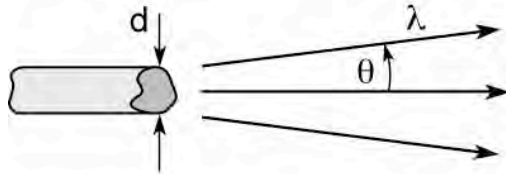
**1  $\mu\text{m}^D$  pinhole**

**25 mm wide CCD  
at 410 mm**

Courtesy of Patrick Naulleau, LBNL.



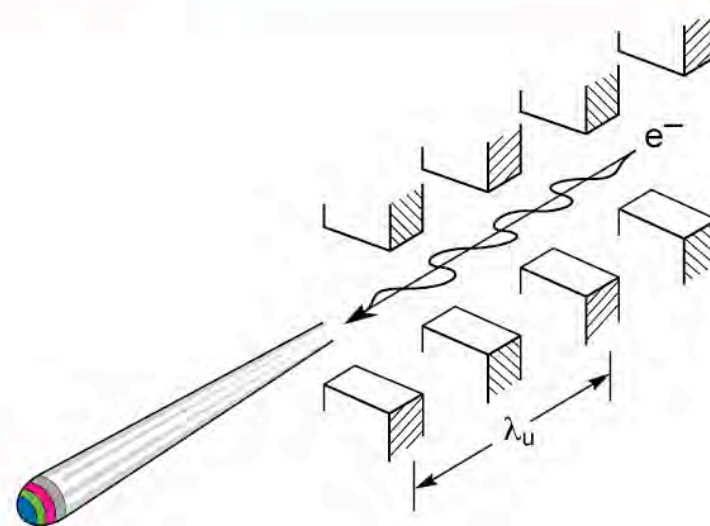
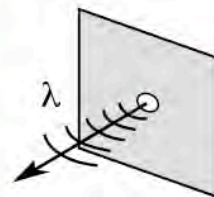
# Coherence at short wavelengths



$$l_{\text{coh}} = \lambda^2 / 2\Delta\lambda \quad \{\text{temporal (longitudinal) coherence}\} \quad (8.3)$$

$$d \cdot \theta = \lambda / 2\pi \quad \{\text{spatial (transverse) coherence}\} \quad (8.5)$$

$$\text{or } d \cdot 2\theta|_{\text{FWHM}} = 0.44 \lambda \quad (8.5^*)$$

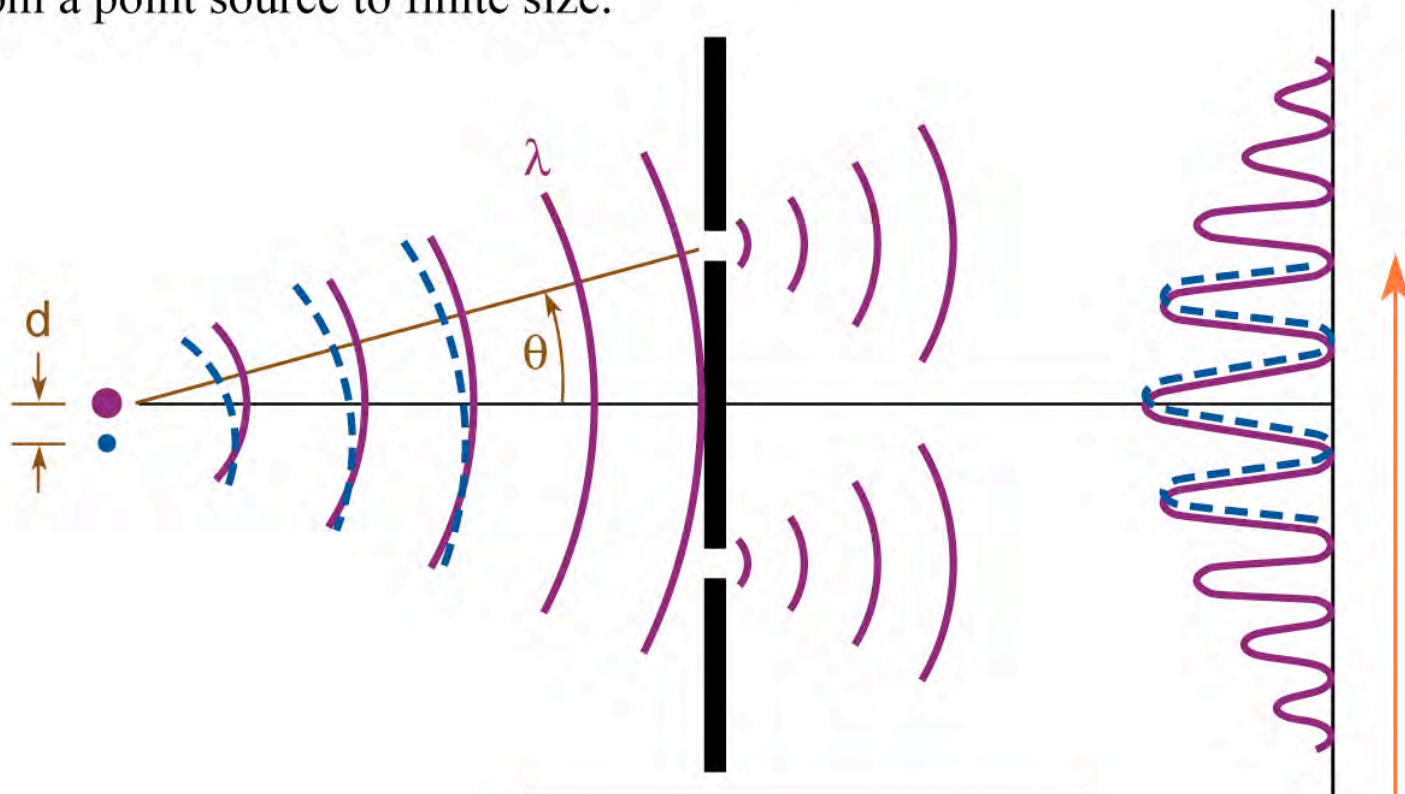


$$\bar{P}_{\text{coh},N} = \frac{(\lambda/2\pi)^2}{(d_x\theta_x)(d_y\theta_y)} \bar{P}_{\text{cen}} \quad (8.6)$$

$$\bar{P}_{\text{coh},\lambda/\Delta\lambda} = \frac{e\lambda_u I \eta (\Delta\lambda/\lambda) N^2}{8\pi\epsilon_0 d_x d_y} \cdot \left[ 1 - \frac{\hbar\omega}{\hbar\omega_0} \right] f(K) \quad (8.9)$$

# Young's double slit experiment: spatial coherence and the persistence of fringes

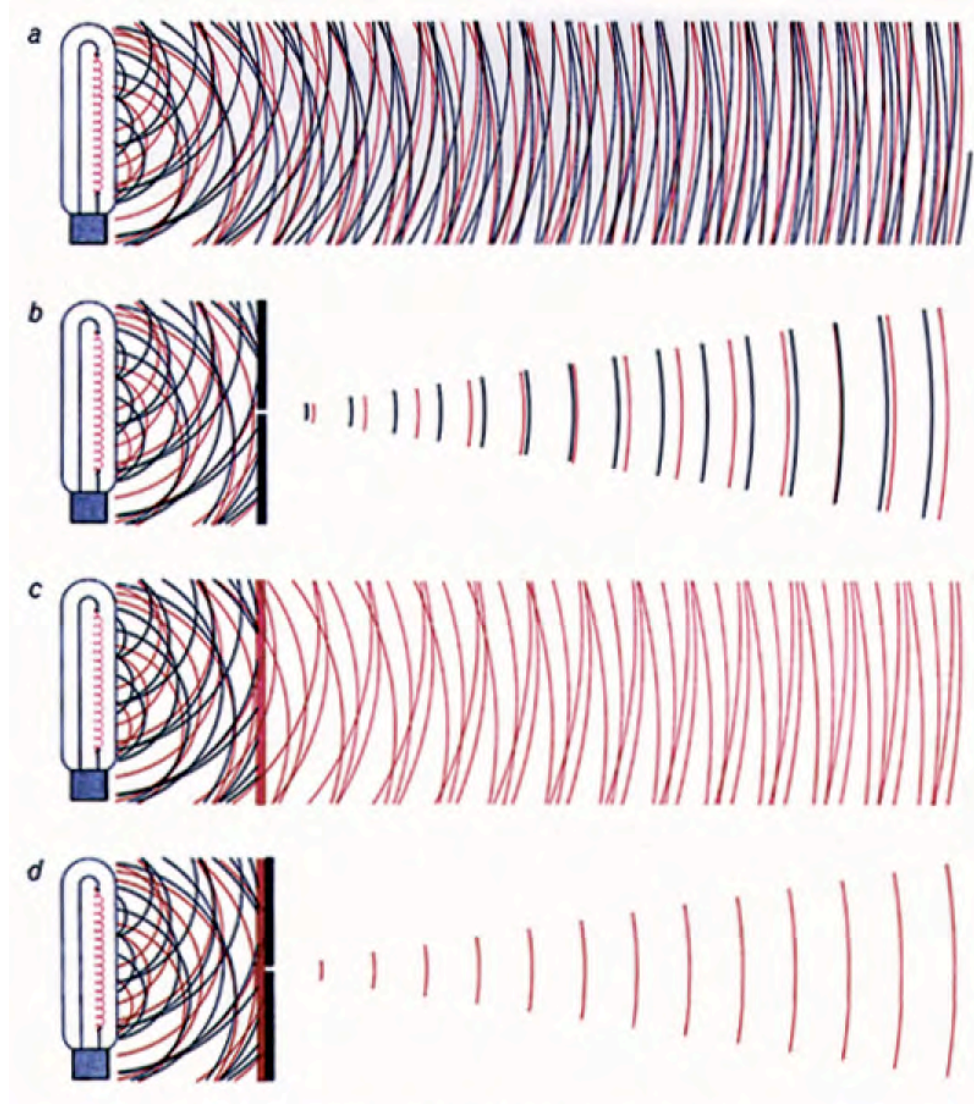
Persistence of fringes as the source grows from a point source to finite size.



$$d \cdot 2\theta|_{\text{FWHM}} \approx \lambda/2$$

$$\lambda_{\text{coh}} = \lambda^2 / 2\Delta\lambda = \frac{1}{2} N_{\text{coh}} \lambda$$

# Spatial and spectral filtering to produce coherent radiation



Courtesy of A. Schawlow, Stanford.

Ch08\_F08.ai



# Spatial and temporal coherence

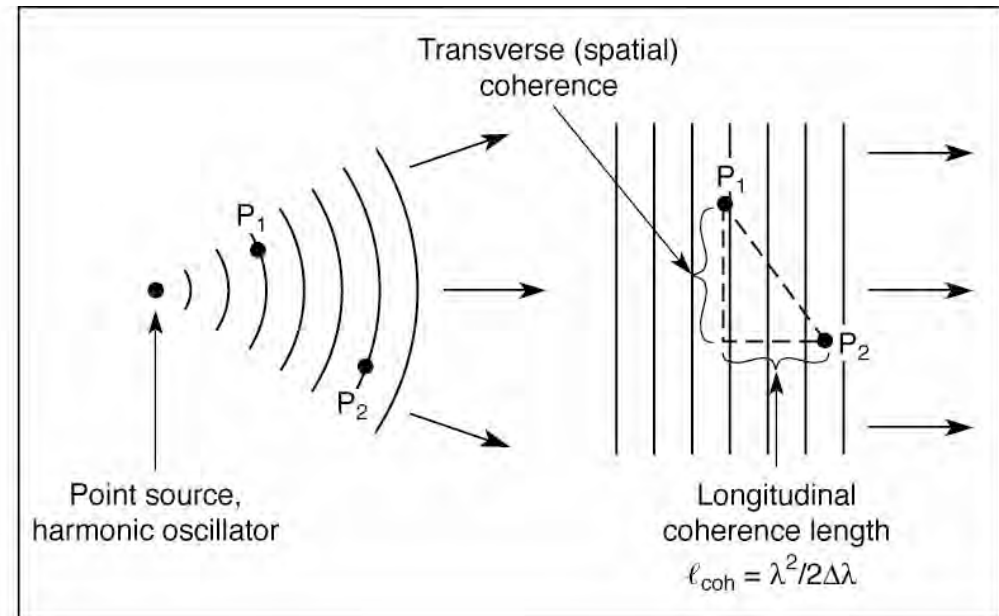
Mutual coherence factor

$$\Gamma_{12}(\tau) \equiv \langle E_1(t + \tau) E_2^*(t) \rangle \quad (8.1)$$

Normalize degree of spatial coherence  
(complex coherence factor)

$$\mu_{12} = \frac{\langle E_1(t) E_2^*(t) \rangle}{\sqrt{\langle |E_1|^2 \rangle} \sqrt{\langle |E_2|^2 \rangle}} \quad (8.12)$$

A high degree of coherence ( $\mu \rightarrow 1$ ) implies an ability to form a high contrast interference (fringe) pattern. A low degree of coherence ( $\mu \rightarrow 0$ ) implies an absence of interference, except with great care. In general radiation is partially coherent.



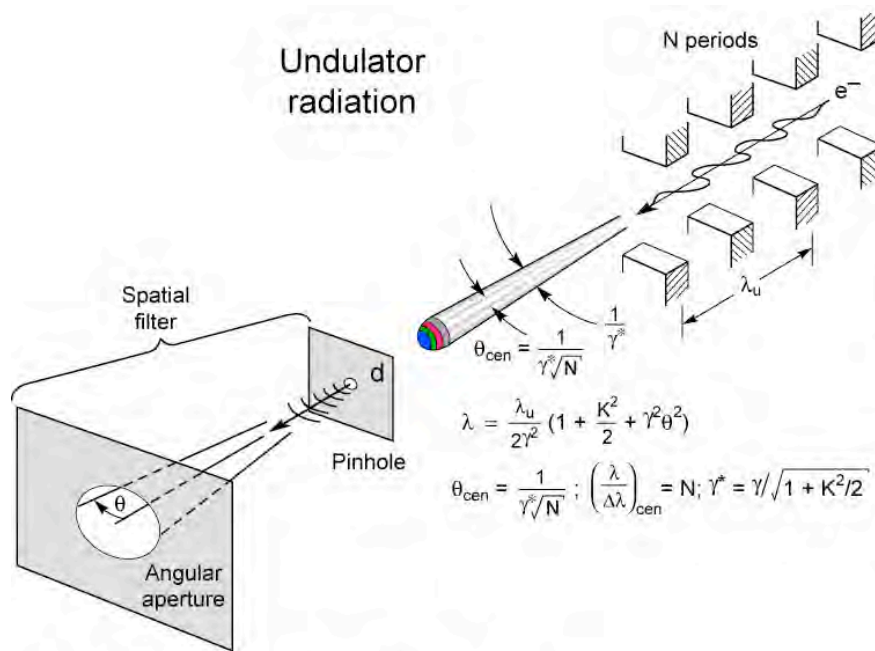
Longitudinal (temporal) coherence length

$$\ell_{\text{coh}} = \frac{\lambda^2}{2 \Delta\lambda} \quad (8.3)$$

Full spatial (transverse) coherence

$$d \cdot \theta = \lambda / 2\pi \quad (8.5)$$

# Spatially filtered undulator radiation

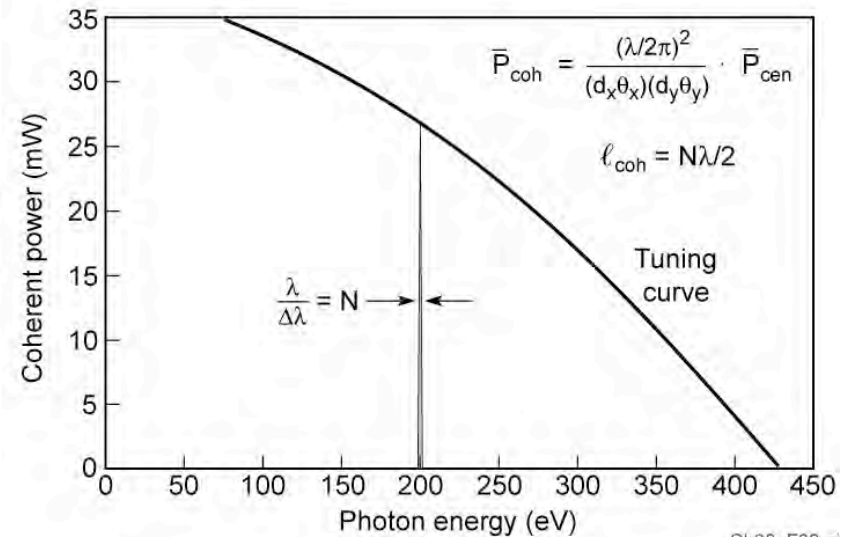
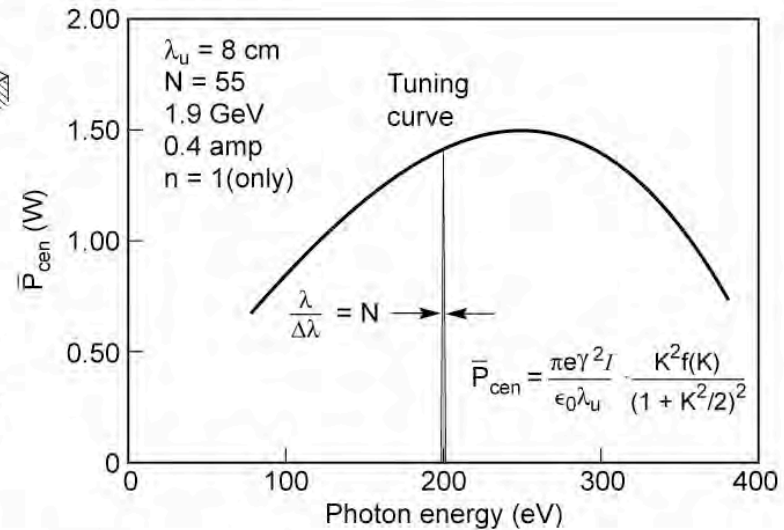


Using a pinhole-aperture spatial filter,  
passing only radiation that satisfies  $d \cdot \theta = \lambda/2\pi$

$$\bar{P}_{coh,N} = \left(\frac{\lambda/2\pi}{d_x \theta_x}\right) \left(\frac{\lambda/2\pi}{d_y \theta_y}\right) \bar{P}_{cen} \quad (8.6)$$

$$\bar{P}_{coh,N} = \frac{e\lambda_u I N}{8\pi \epsilon_0 d_x d_y} \left(1 - \frac{\hbar\omega}{\hbar\omega_0}\right) f(\hbar\omega/\hbar\omega_0) \quad (8.9)$$

for  $d_x = 2\sigma_x$ ,  $d_y = 2\sigma_y$ ,  $\theta_{Tx} \rightarrow \theta_x$ ,  $\theta_{Ty} \rightarrow \theta_y$ ,  
and  $\sigma'^2 \ll \theta_{cen}^2$ .



Ch08\_F09.ai





## Spatial and spectral filtering of undulator radiation



In addition to the pinhole – angular aperture for spatial filtering and spatial coherence, add a monochromator for narrowed bandwidth and increased temporal coherence:

$$\bar{P}_{\text{coh}, \lambda / \Delta \lambda} = \underbrace{\eta}_{\text{beamline efficiency}} \underbrace{\frac{(\lambda / 2 \pi)^2}{(d_x \theta_x)(d_y, \theta_y)}}_{\text{spatial filtering}} \cdot \underbrace{N \frac{\Delta \lambda}{\lambda}}_{\text{spectral filtering}} \cdot \bar{P}_{\text{cen}} \quad (8.10a)$$

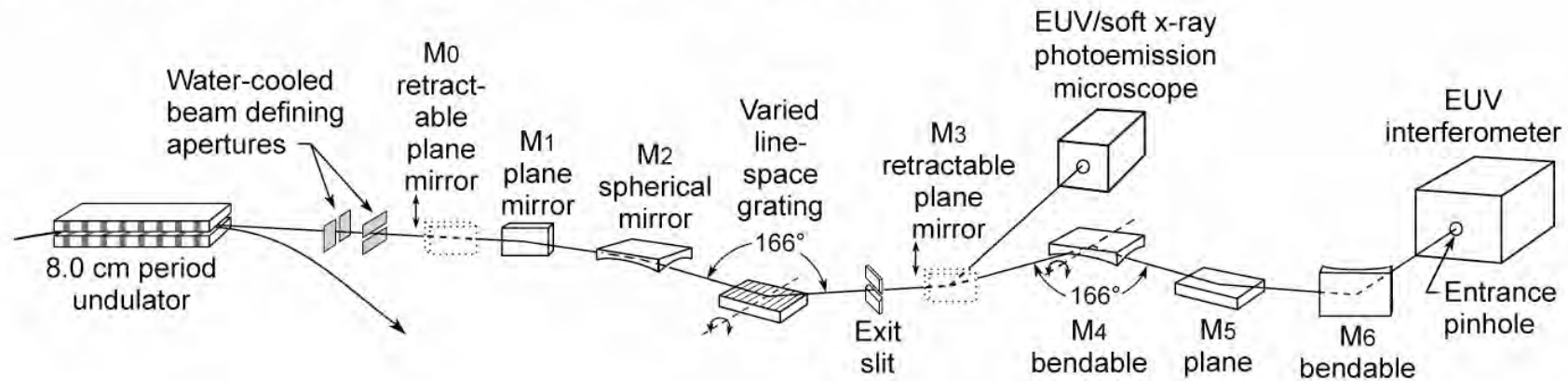
which for  $\sigma'_{x,y} \ll \theta_{\text{cen}}^2$  (the undulator condition) gives the spatially and temporally coherent power ( $d \cdot \theta = \lambda / 2 \pi$  ;  $l_{\text{coh}} = \frac{\lambda^2}{2 \Delta \lambda}$ )

$$\bar{P}_{\text{coh}, \lambda / \Delta \lambda} = \frac{e \lambda_u I \eta (\Delta \lambda / \lambda) N^2}{8 \pi \epsilon_0 d_x d_y} \cdot \left( 1 - \frac{\hbar \omega}{\hbar \omega_0} \right) f(\hbar \omega / \hbar \omega_0) \quad (8.10c)$$

which we note scales as  $N^2$ .

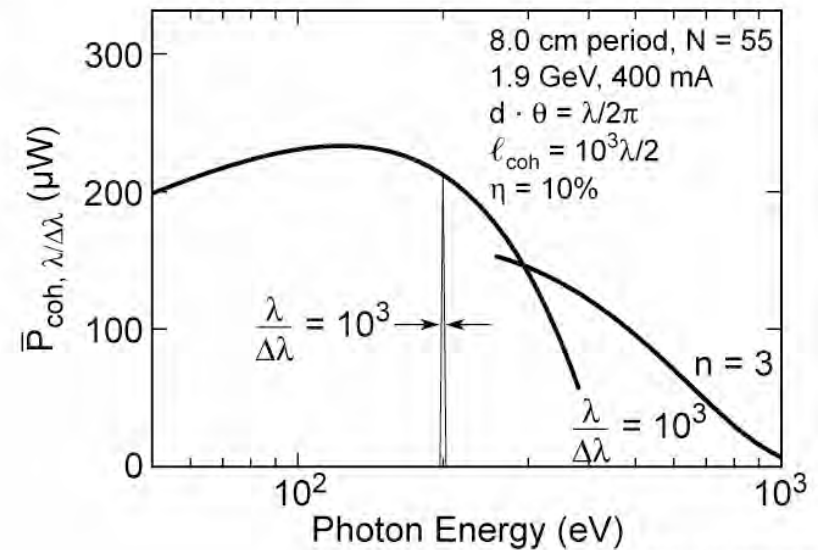
# Spatially and spectrally filtered undulator radiation

- Pinhole filtering for full spatial coherence
- Monochromator for spectral filtering to  $\lambda/\Delta\lambda > N$



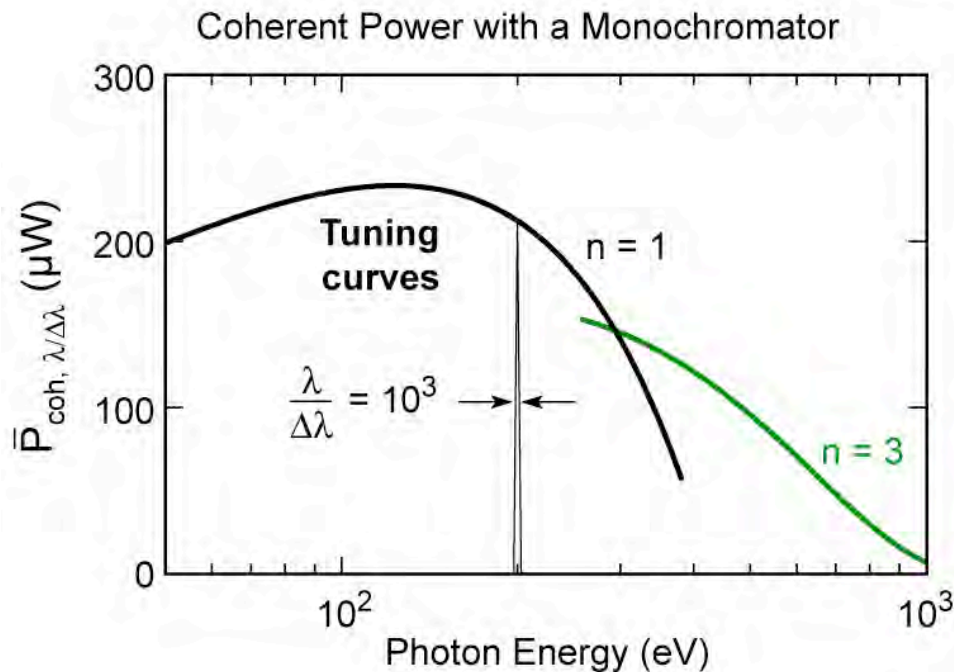
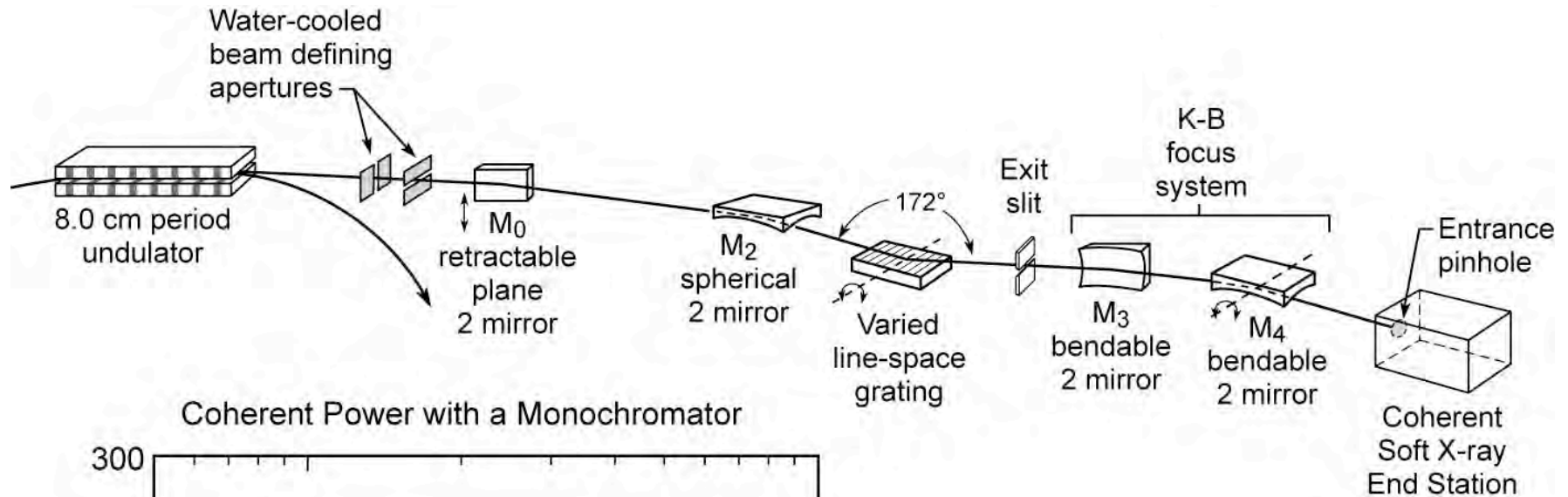
$$\bar{P}_{\text{coh}, \lambda/\Delta\lambda} = \underbrace{\eta}_{\text{beamline efficiency}} \underbrace{\frac{(\lambda/2\pi)^2}{(d_x \theta_x)(d_y \theta_y)}}_{\text{spatial filtering}} \cdot \underbrace{N \frac{\Delta\lambda}{\lambda}}_{\text{spectral filtering}} \cdot \bar{P}_{\text{cen}} \quad (8.10a)$$

$$\bar{P}_{\text{coh}, \lambda/\Delta\lambda} = \frac{e\lambda_u I \eta (\Delta\lambda/\lambda) N^2}{8\pi \epsilon_0 d_x d_y} \cdot \left(1 - \frac{\hbar\omega}{\hbar\omega_0}\right) f(\hbar\omega/\hbar\omega_0) \quad (\sigma'^2 \ll \theta_{\text{cen}}^2) \quad (8.10c)$$



Ch08\_F11\_Mar08.ai

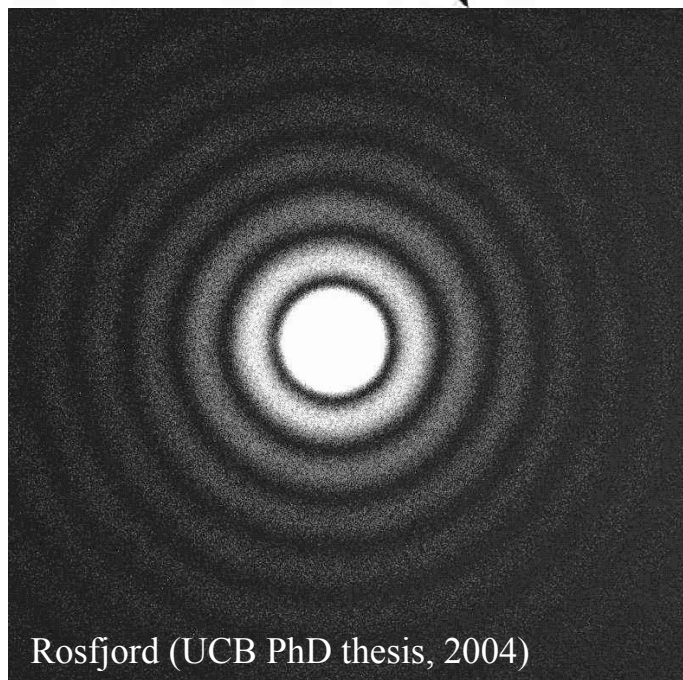
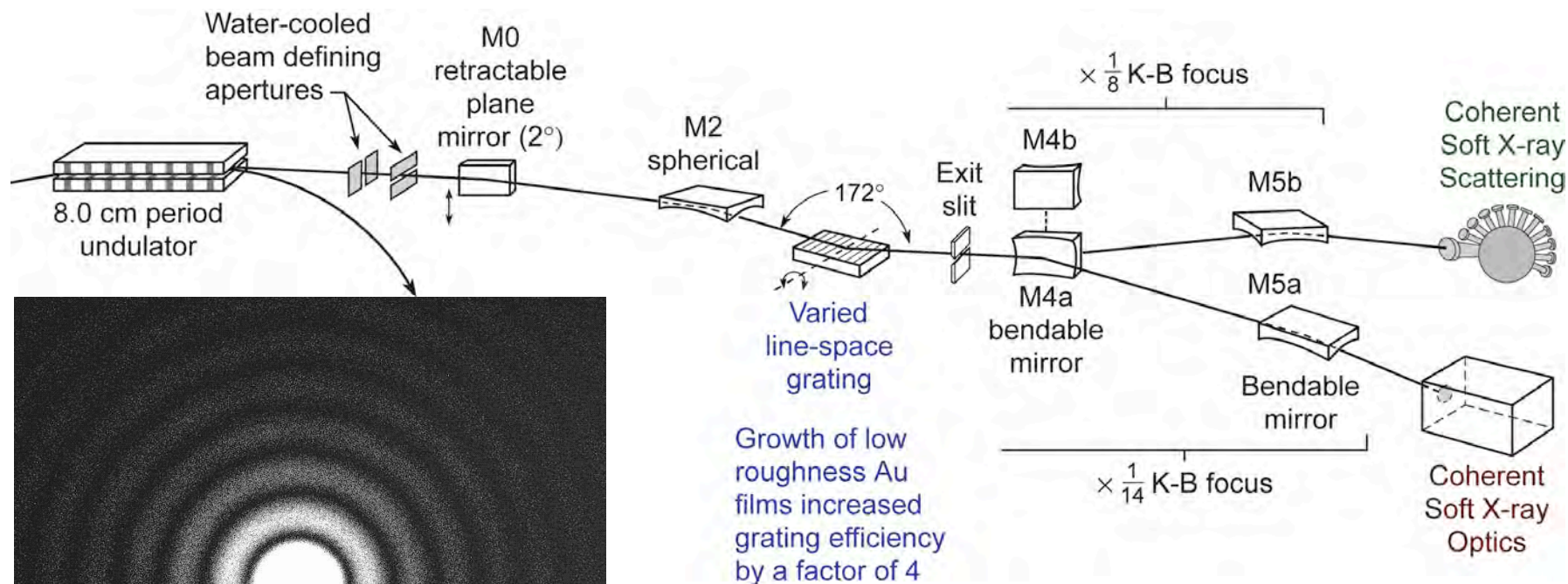
# Coherent soft x-ray beamline: use of a higher harmonic ( $n = 3$ ) to access shorter wavelengths



8.0 cm period,  $N = 55$   
 1.9 GeV, 400 mA  
 $d \cdot \theta = \lambda/2\pi$   
 $\ell_{\text{coh}} = 1000 \lambda/2$   
 $\eta_{\text{euv}} = 10\%$ ,  $\eta_{\text{srx}} = 10\%$



# Coherent soft x-ray science beamline



Rosfjord (UCB PhD thesis, 2004)

K. Rosfjord, Y. Liu, D. Attwood, "Tunable Coherent Soft X-Rays", IEEE J. Sel. Top. Quant. Electr. **10**, 1405 (Nov/Dec 2004)

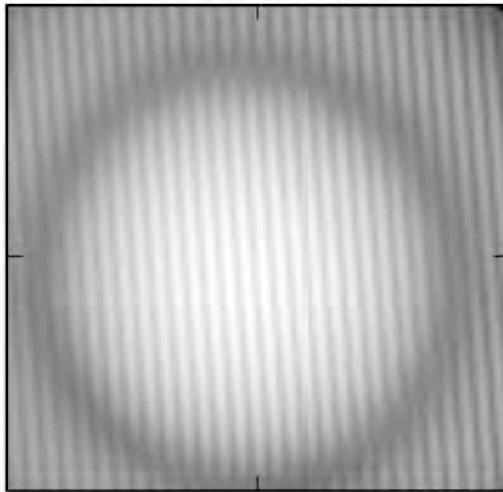
Energy range 200-1000eV

Coherent flux at 600 eV:  
 $2 \times 10^{11}$  ph/sec/0.1%BW

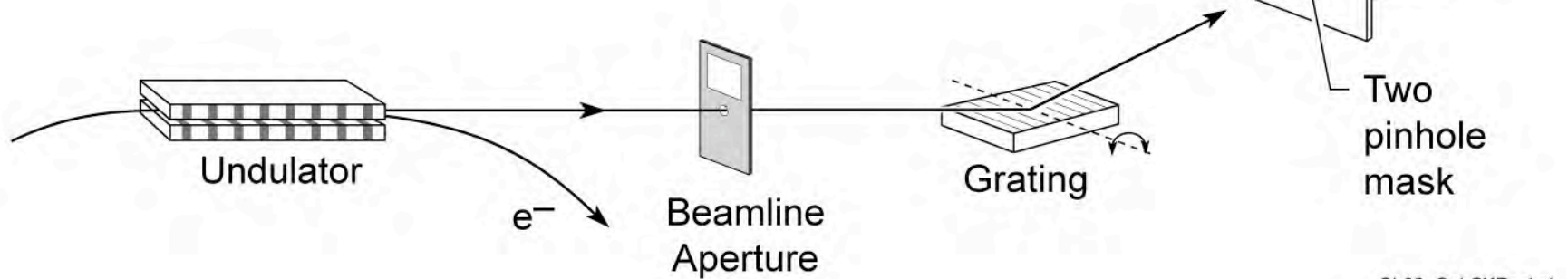
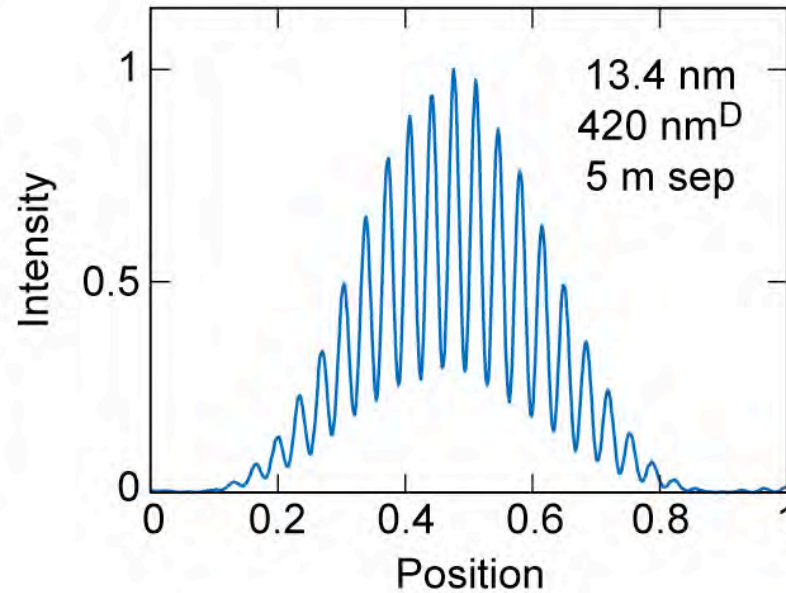
$\lambda = 2.07$  nm (600 eV)

- Wavefront interferometry to measure aberrations in zone plate lenses
- Measure material properties ( $f_1$  &  $f_2$ )
- Develop new coherent soft x-ray optical techniques (Fourier Optics)
- Coherent scattering from magnetic nanostructures

# Undulator beamline for high spatial coherence measurements



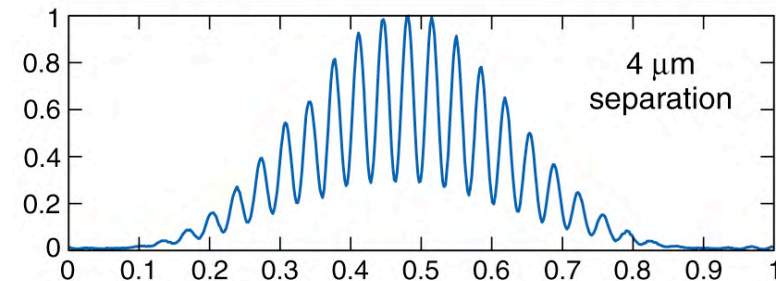
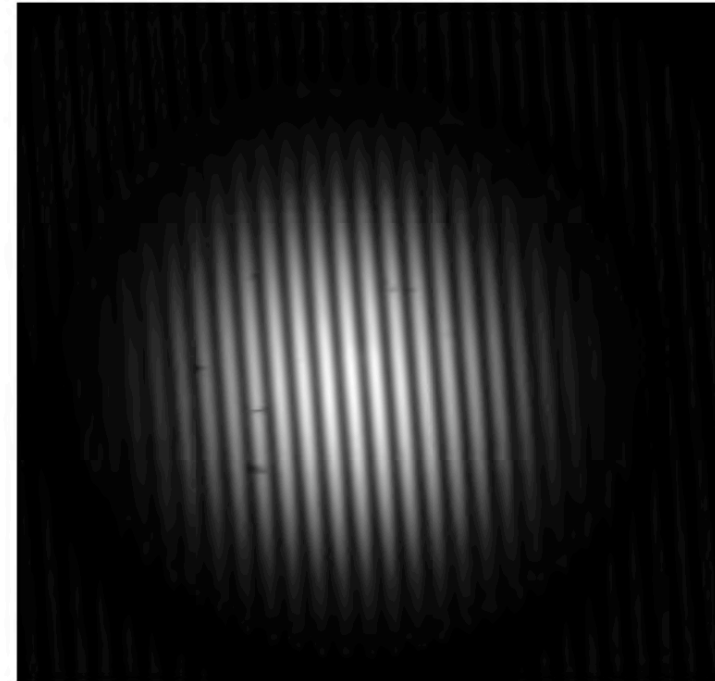
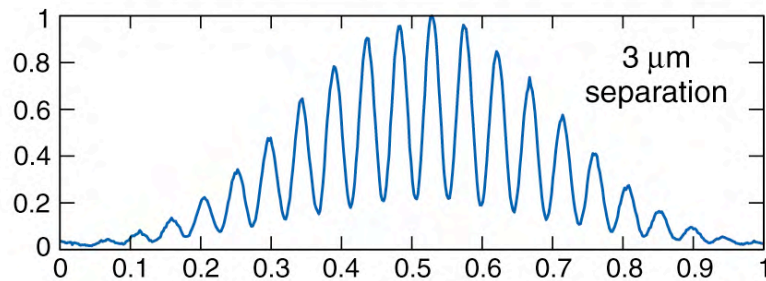
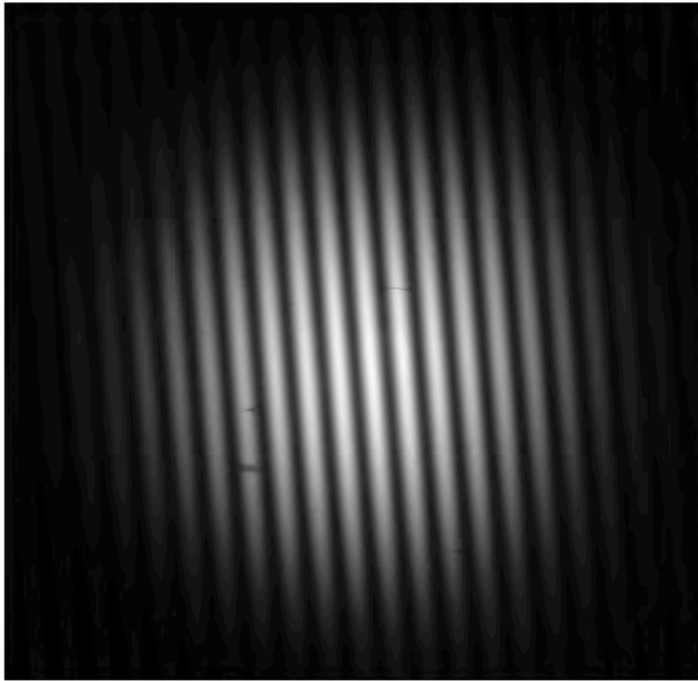
C. Chang



Ch08\_CohSXRsci.ai



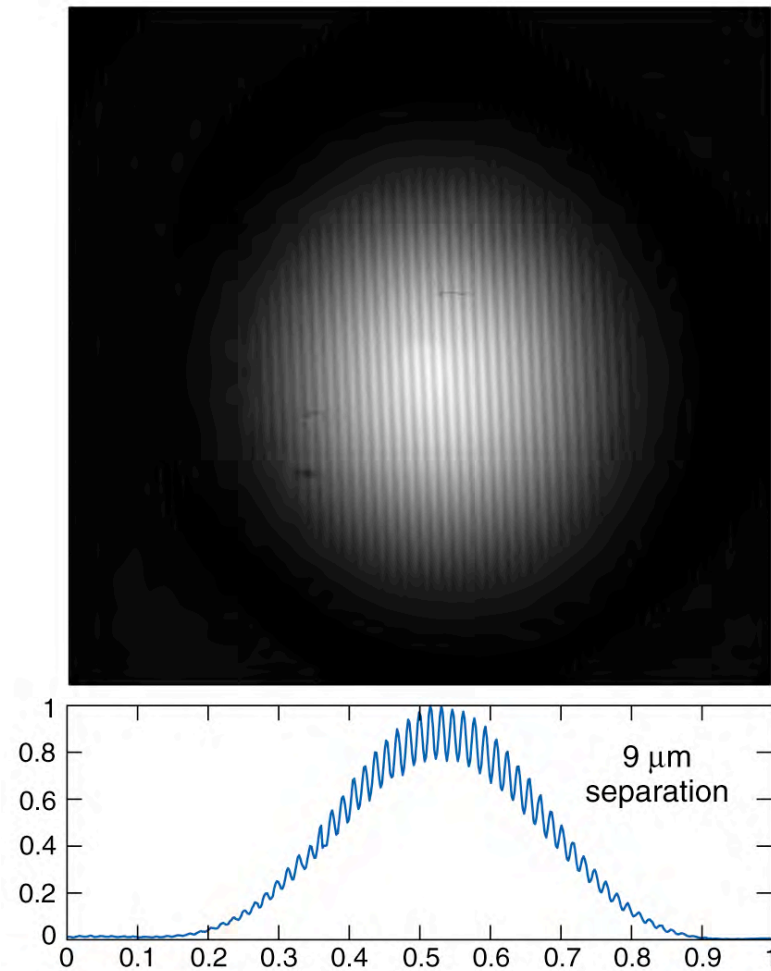
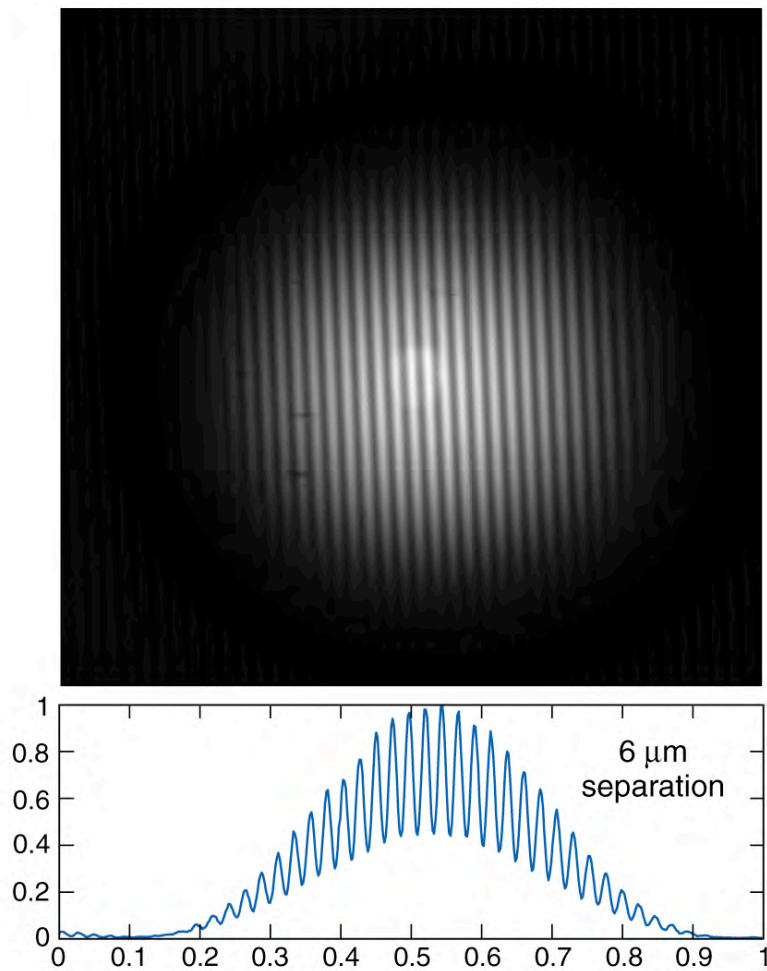
# Spatial coherence measurements of undulator radiation using the classic 2-pinhole technique



Courtesy of Chang Chang, UC Berkeley and LBNL.

$\lambda = 13.4$  nm, 450 nm diameter pinholes, 1024 x 1024 EUV/CCD at 26 cm ALS, 1.9 GeV,  $\lambda_u = 8$  cm,  $N = 55$

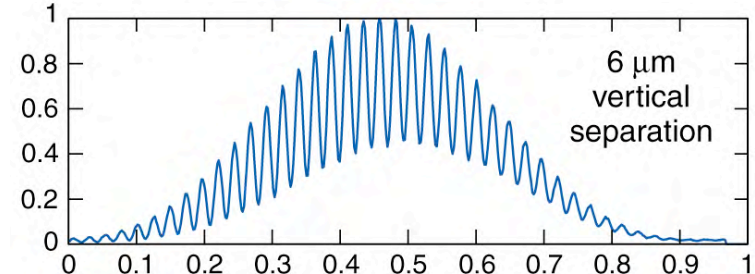
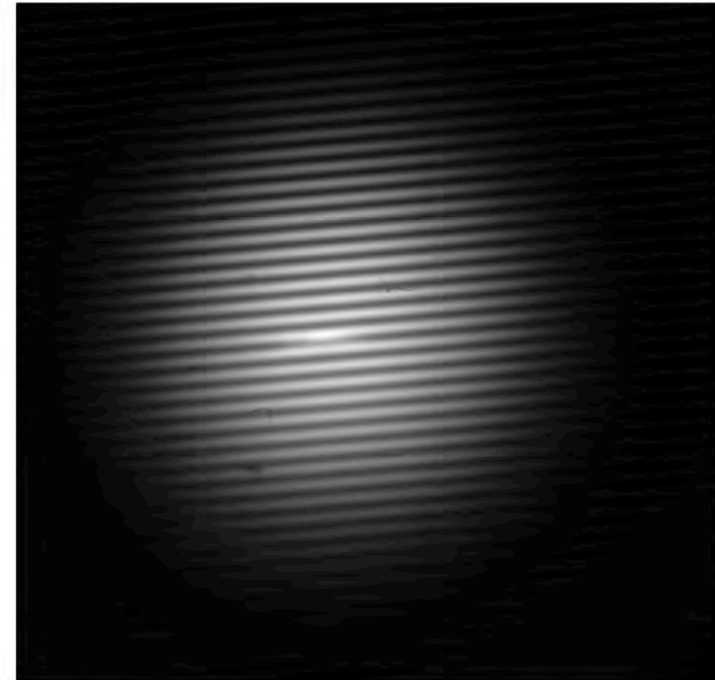
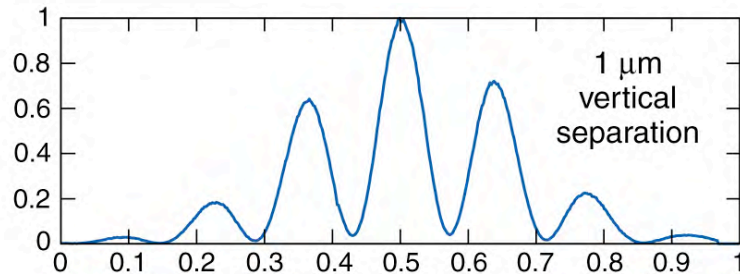
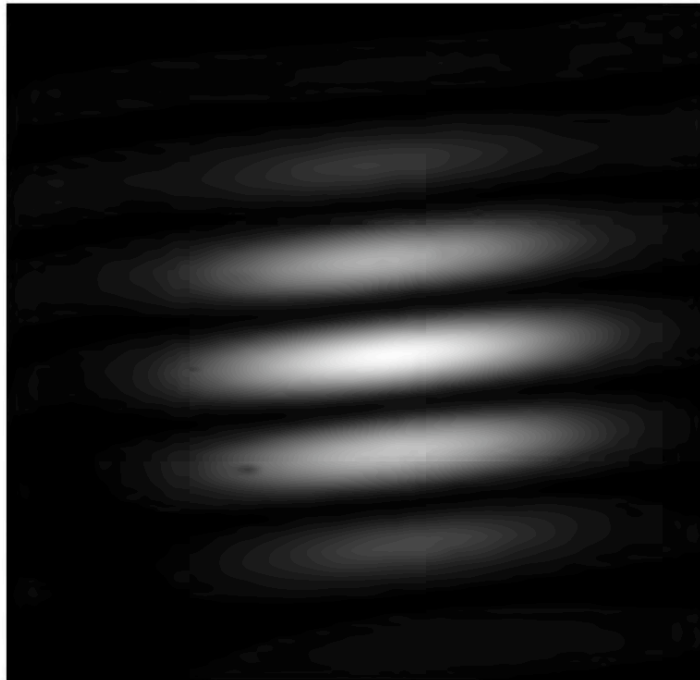
# Spatial coherence measurements of undulator radiation using the classic 2-pinhole technique



Courtesy of Chang Chang, UC Berkeley and LBNL.

$\lambda = 13.4$  nm, 450 nm diameter pinholes, 1024 x 1024 EUV/CCD at 26 cm ALS, 1.9 GeV,  $\lambda_u = 8$  cm,  $N = 55$

# Spatial coherence measurements in the vertical plane

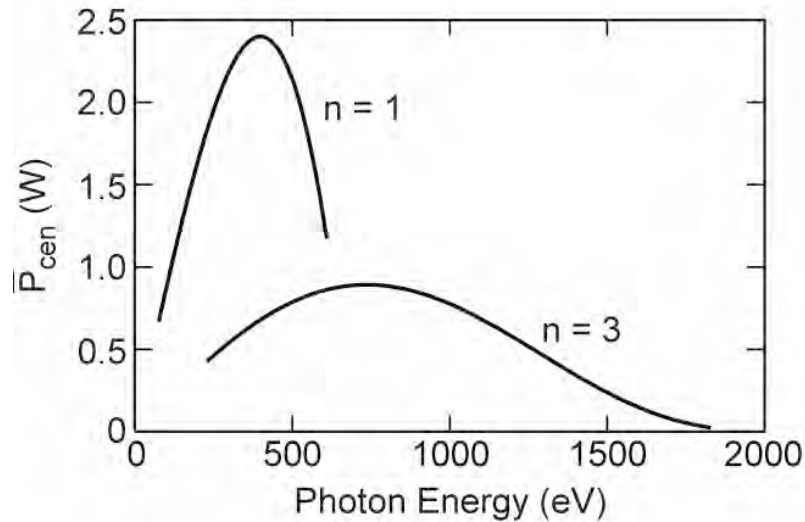


Courtesy of Chang Chang, UC Berkeley and LBNL.

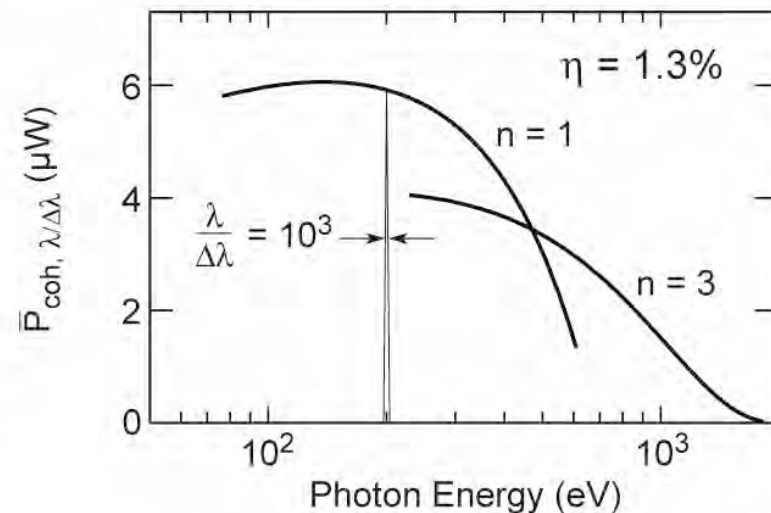
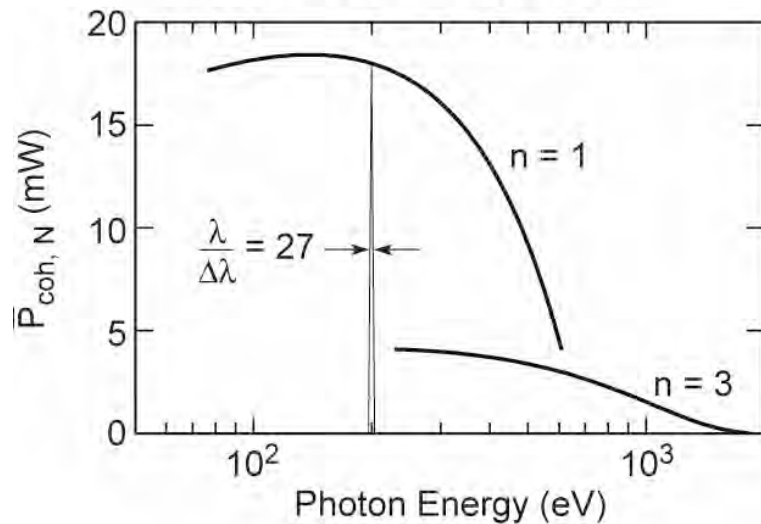
$\lambda = 13.4$  nm, 450 nm diameter pinholes, 1024 x 1024 EUV/CCD at 26 cm ALS, 1.9 GeV,  $\lambda_u = 8$  cm,  $N = 55$

# Coherent power for an EPU at the ALS

## U5 EPU



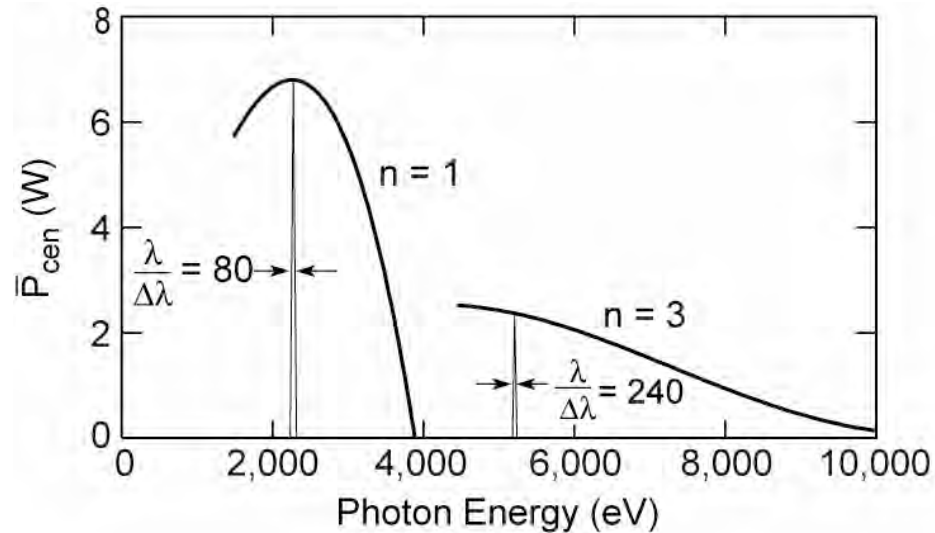
1.9 GeV, 400 mA  
 $\lambda_u = 50$  mm,  $N = 27$   
 $0.5 \leq K \leq 4.0$   
 $\sigma_x = 260$   $\mu$ m,  $\sigma_x' = 23$   $\mu$ r  
 $\sigma_y = 16$   $\mu$ m,  $\sigma_y' = 3.9$   $\mu$ r  
 $\theta_{cen} = 61$   $\mu$ r @  $K = 0.87$  (500 eV)



Ch08\_ALS\_U5epu\_Feb07.ai



# Coherent power at the Australian Synchrotron



3.0 GeV, 200 mA

$\lambda_u = 22$  mm,  $N = 80$

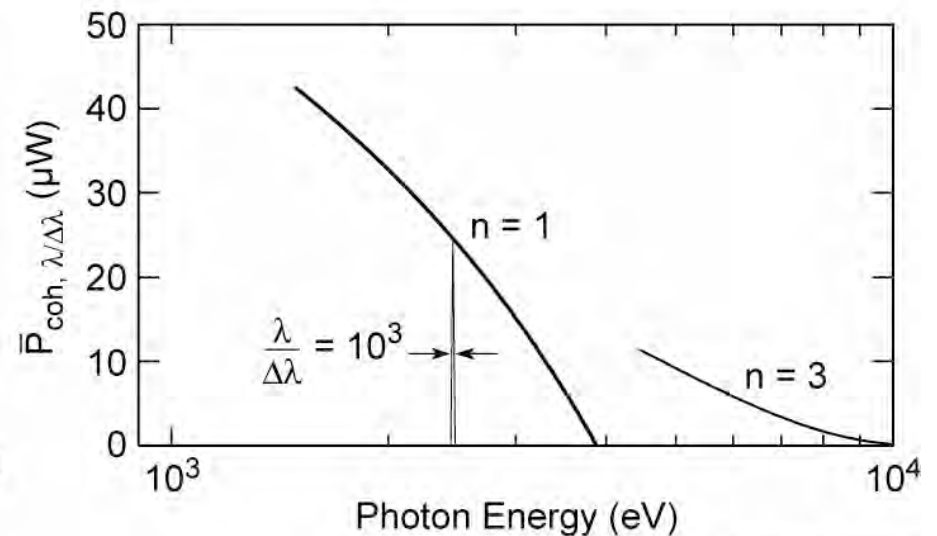
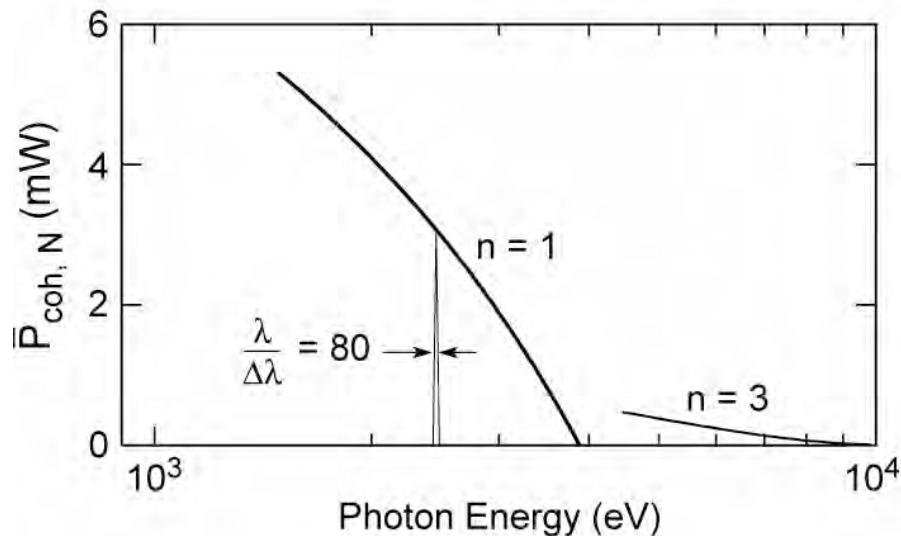
$0 \leq K \leq 1.8$

$\sigma_x = 320$   $\mu\text{m}$ ,  $\sigma_x' = 34$   $\mu\text{rad}$

$\sigma_y = 16$   $\mu\text{m}$ ,  $\sigma_y' = 6$   $\mu\text{rad}$

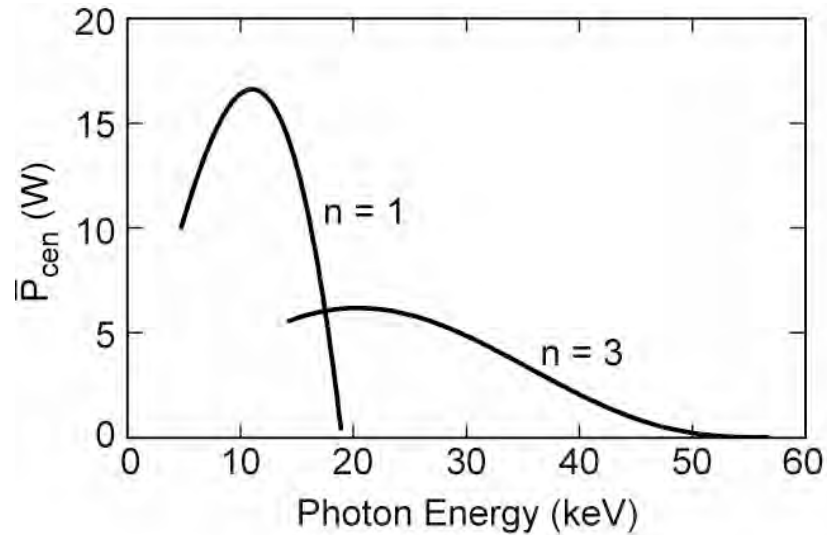
$\theta_{\text{cen}} = 23$   $\mu\text{rad}$  @  $K = 1$

$\eta = 10\%$

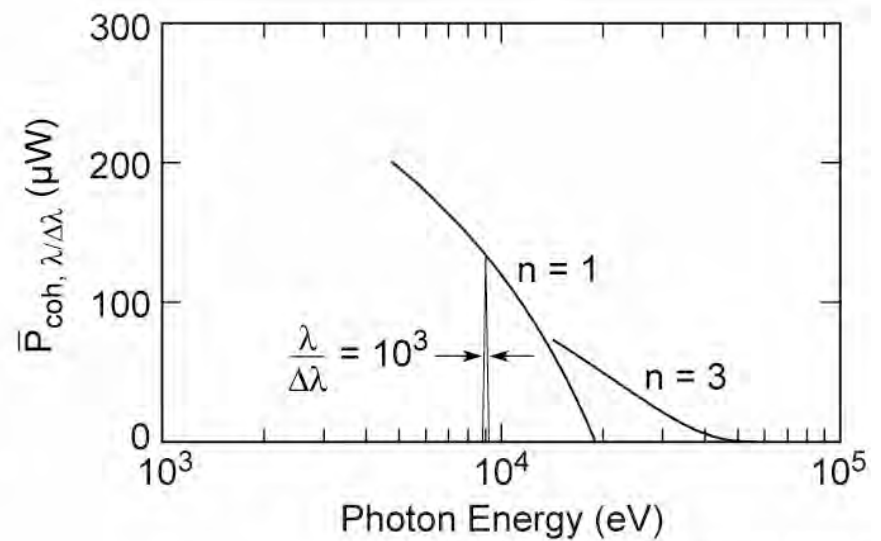
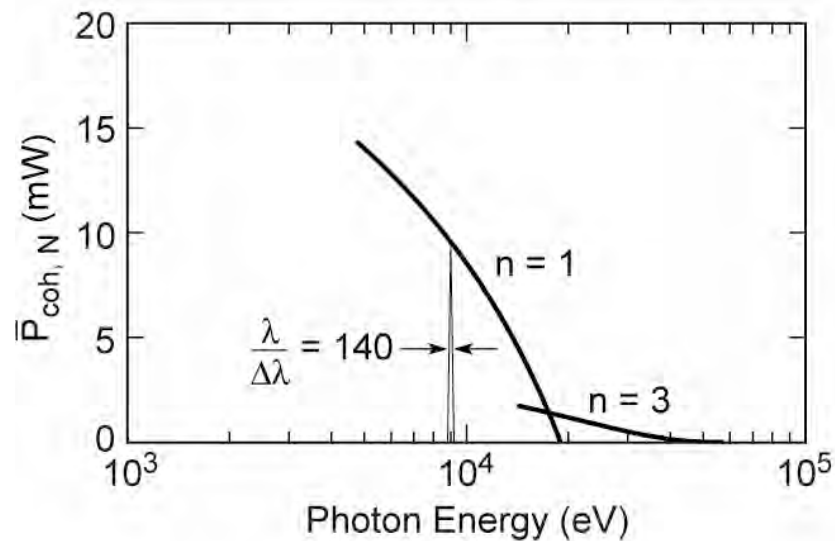


CohPwr\_AustralSynch\_Feb07.ai

# Coherent power at SPring-8

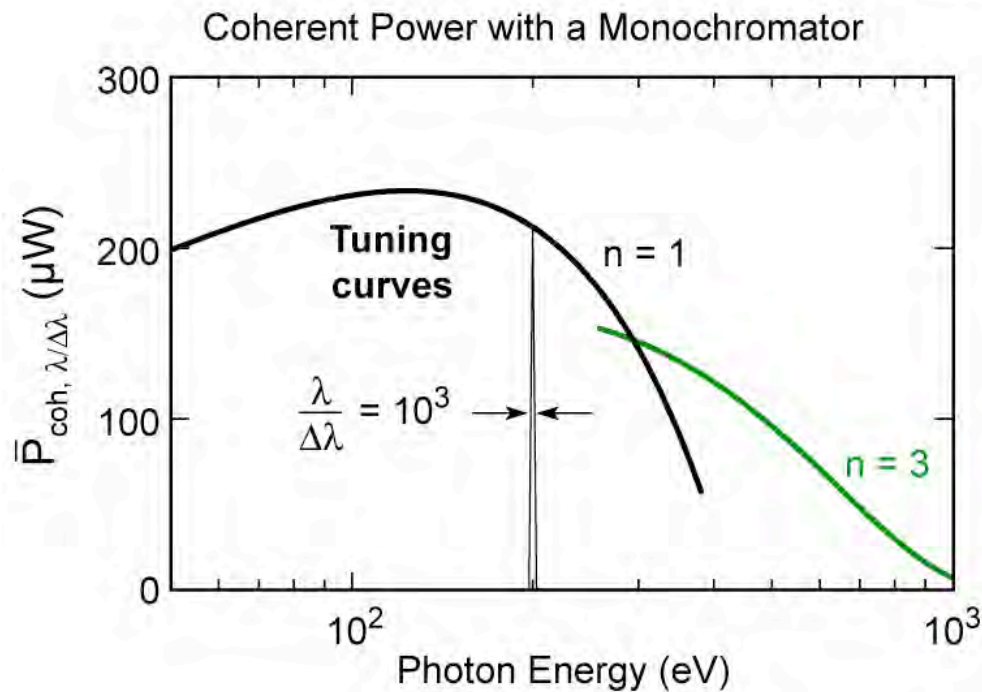
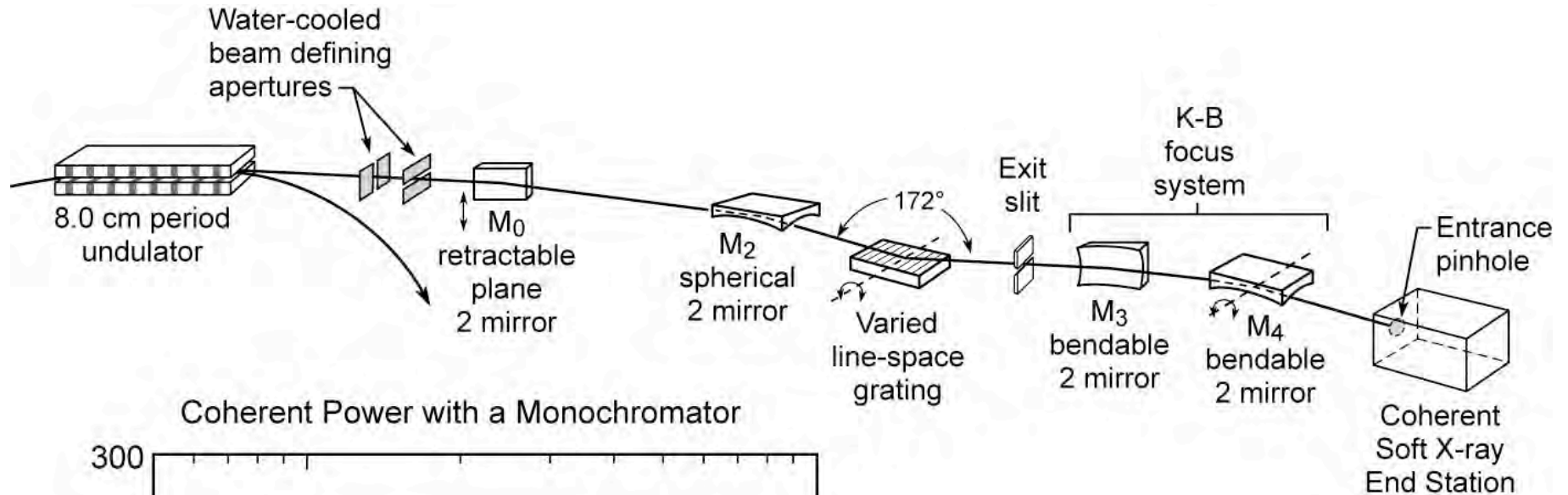


8 GeV, 100 mA  
 $\lambda_u = 32$  mm,  $N = 140$   
 $0 \leq K \leq 2.46$   
 $\sigma_x = 393$   $\mu\text{m}$ ,  $\sigma_x' = 15.7$   $\mu\text{r}$   
 $\sigma_y = 4.98$   $\mu\text{m}$ ,  $\sigma_y' = 1.24$   $\mu\text{r}$   
 $\eta = 10\%$



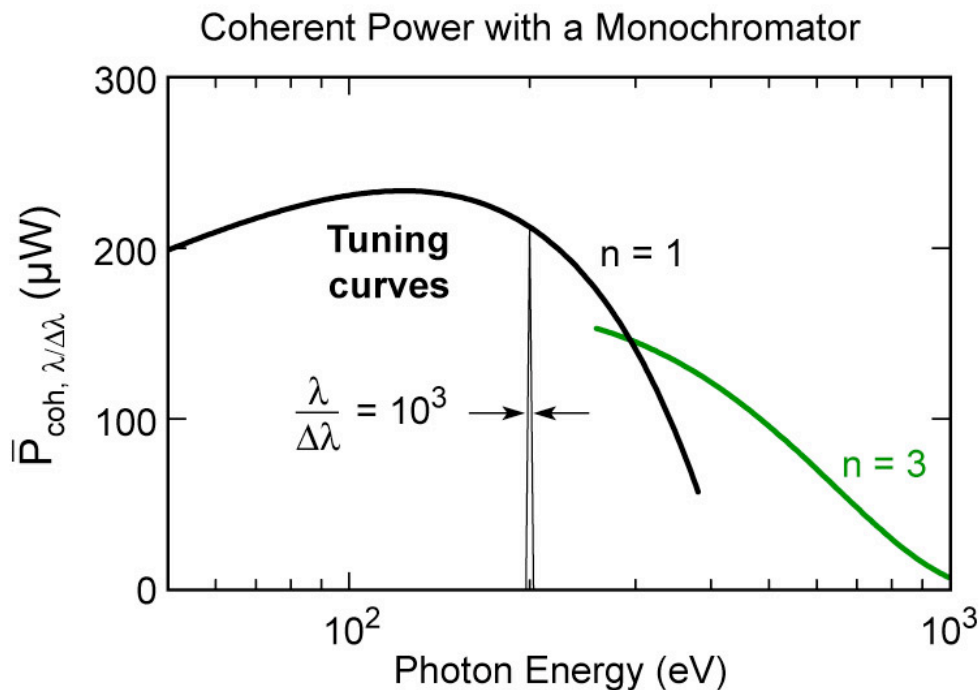
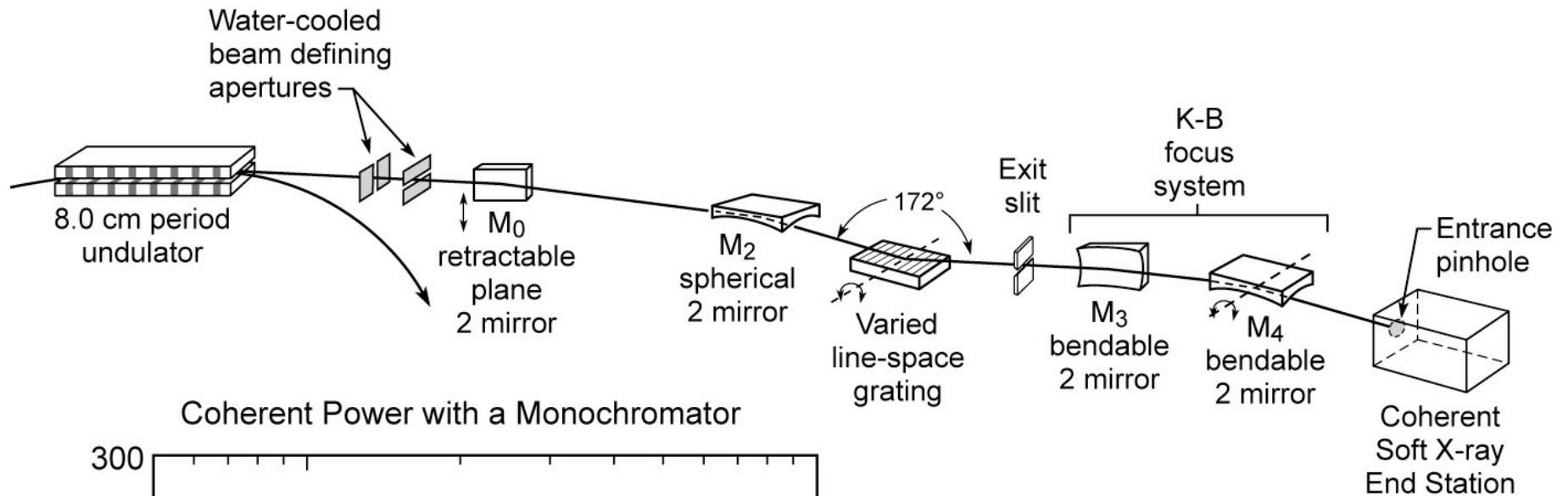
Ch08\_SPring8\_Feb07.ai

# Coherent soft x-ray beamline: use of a higher harmonic ( $n = 3$ ) to access shorter wavelengths



8.0 cm period,  $N = 55$   
 1.9 GeV, 400 mA  
 $d \cdot \theta = \lambda/2\pi$   
 $\ell_{\text{coh}} = 1000 \lambda/2$   
 $\eta_{\text{euv}} = 10\%$ ,  $\eta_{\text{sxr}} = 10\%$

# Coherent soft x-ray beamline: use of a higher harmonic ( $n = 3$ ) to access shorter wavelengths

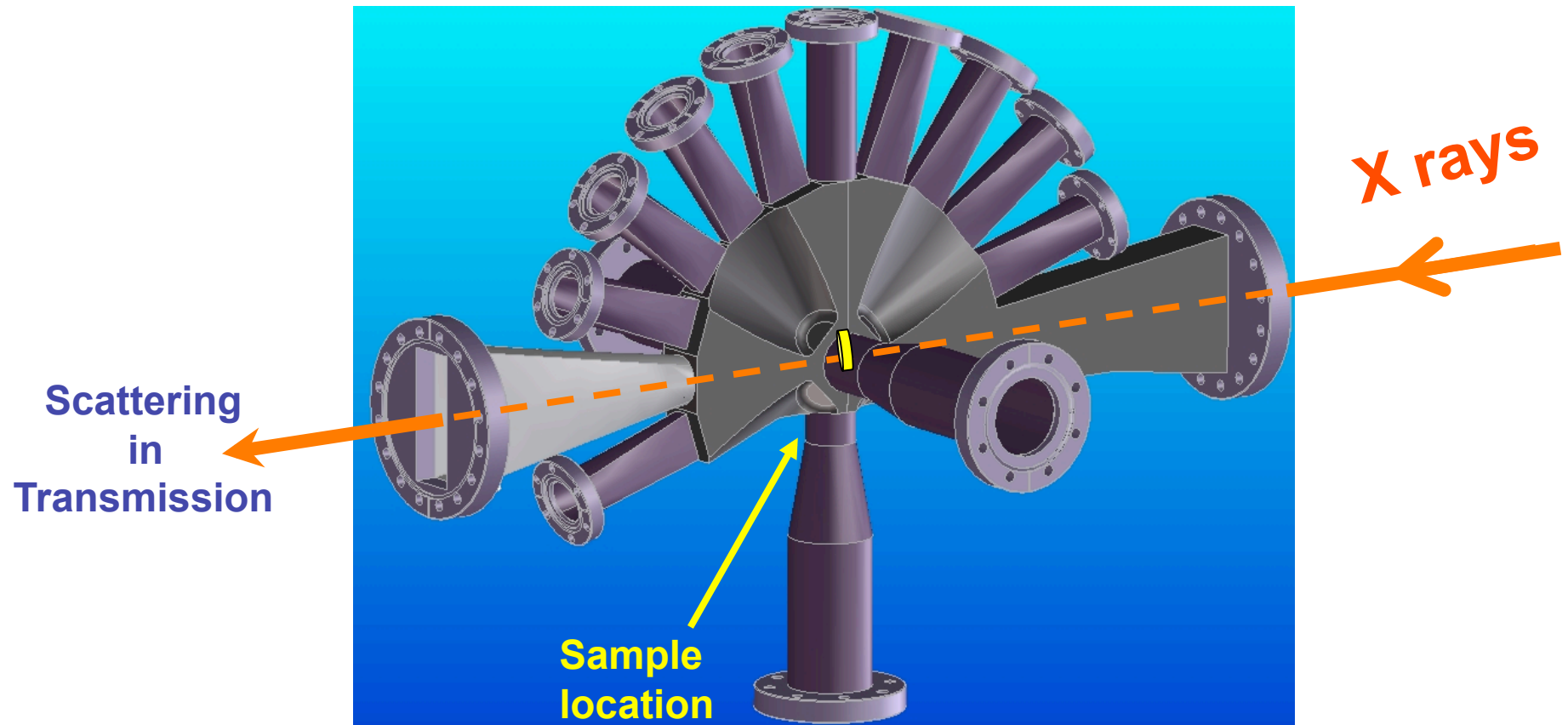


8.0 cm period,  $N = 55$   
 1.9 GeV, 400 mA  
 $d \cdot \theta = \lambda/2\pi$   
 $\ell_{\text{coh}} = 1000 \lambda/2$   
 $\eta_{\text{euv}} = 10\%$ ,  $\eta_{\text{srx}} = 10\%$



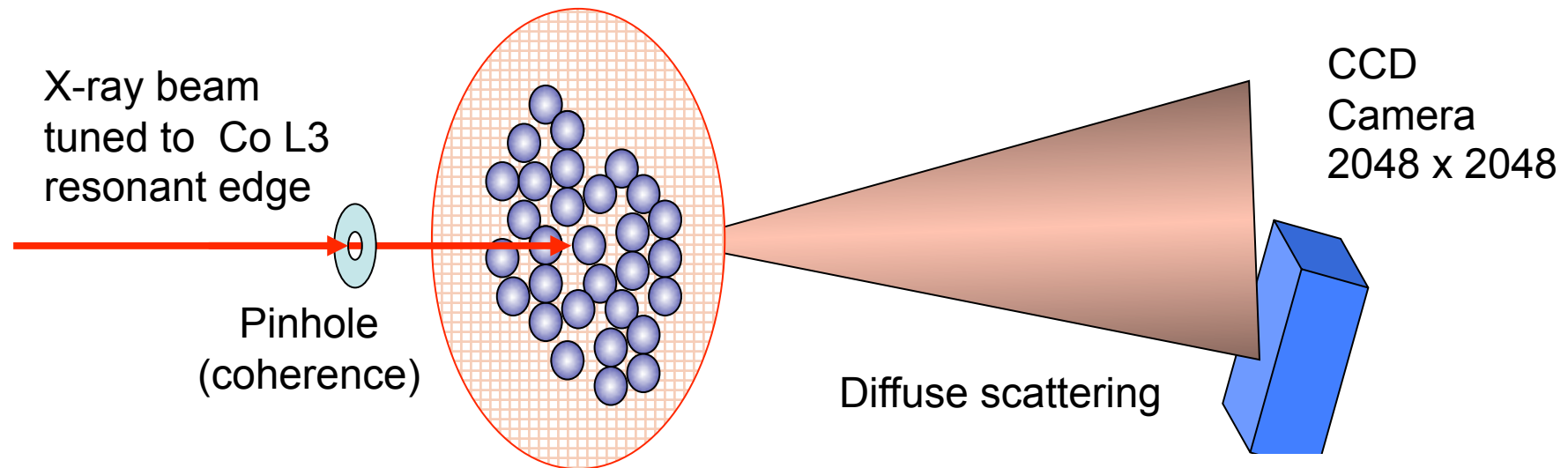
# Coherent Soft X-Ray Magnetic Scattering Endstation

## *Flangosaurus*



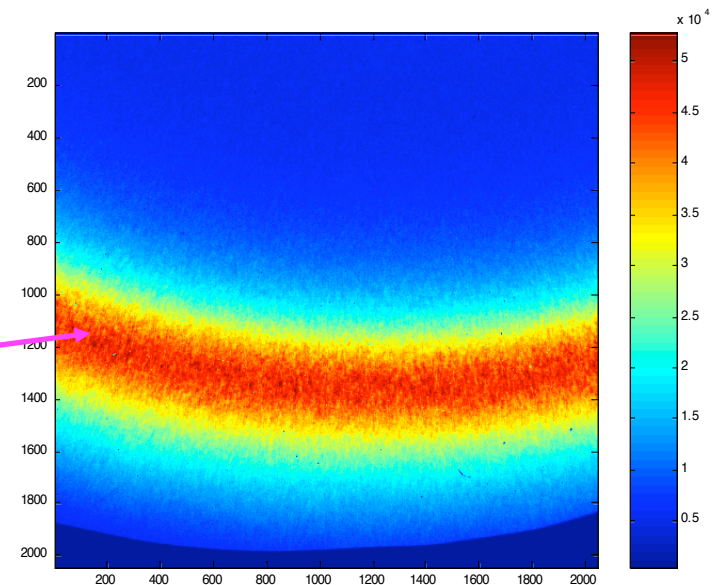
Courtesy of K.Chesnel, S. Kevan, U. Oregon

# Example of experiment in transmission: coherent scattering from nanoparticles

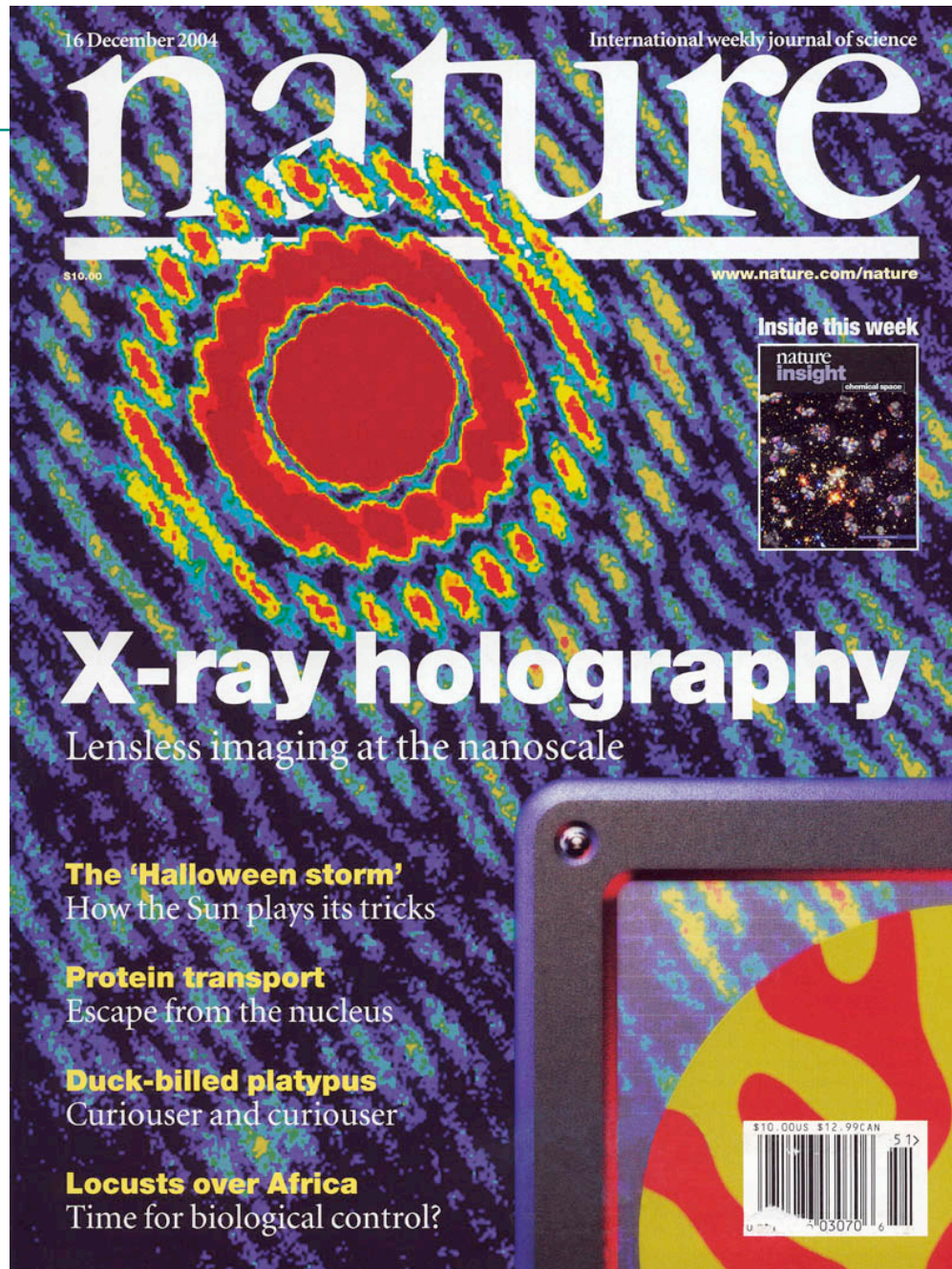


Co Nanoparticles assembly  
precipitated on TEM grid

Scattering ring  
related to  
interparticle distance  
 $\sim 12$  nm

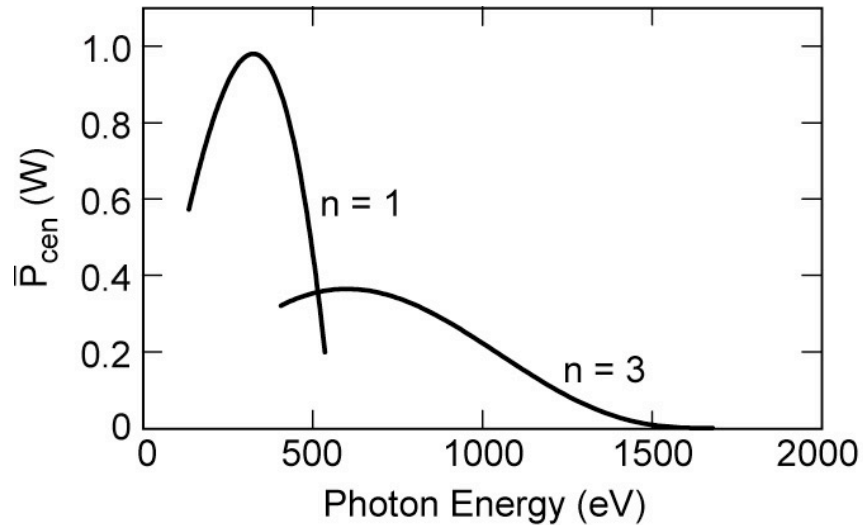


Courtesy of K.Chesnel, S. Kevan, U. Oregon

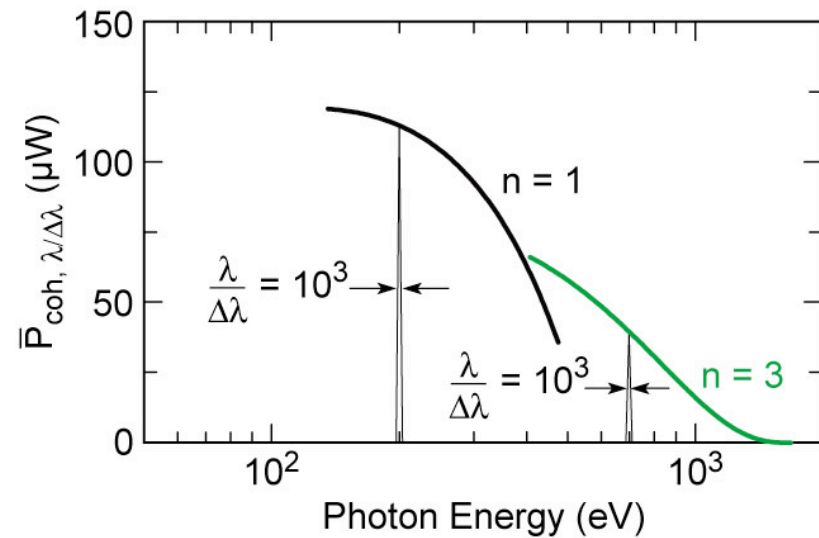
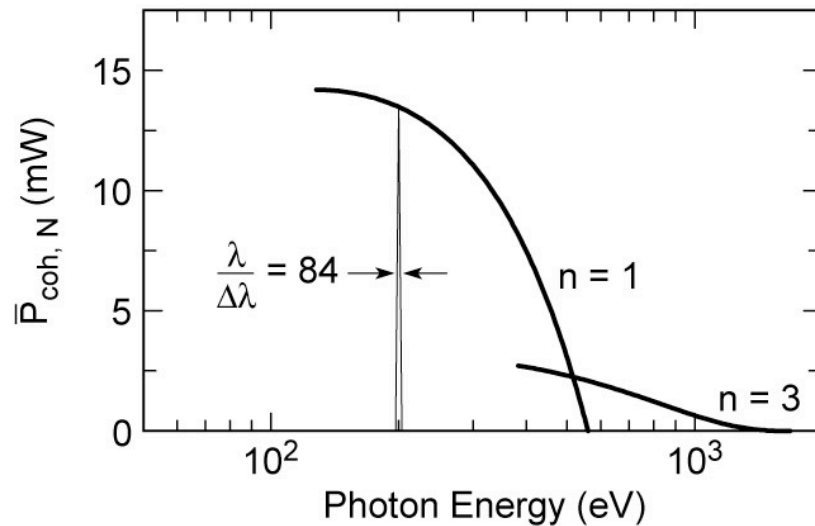




# Coherent power at BESSY II



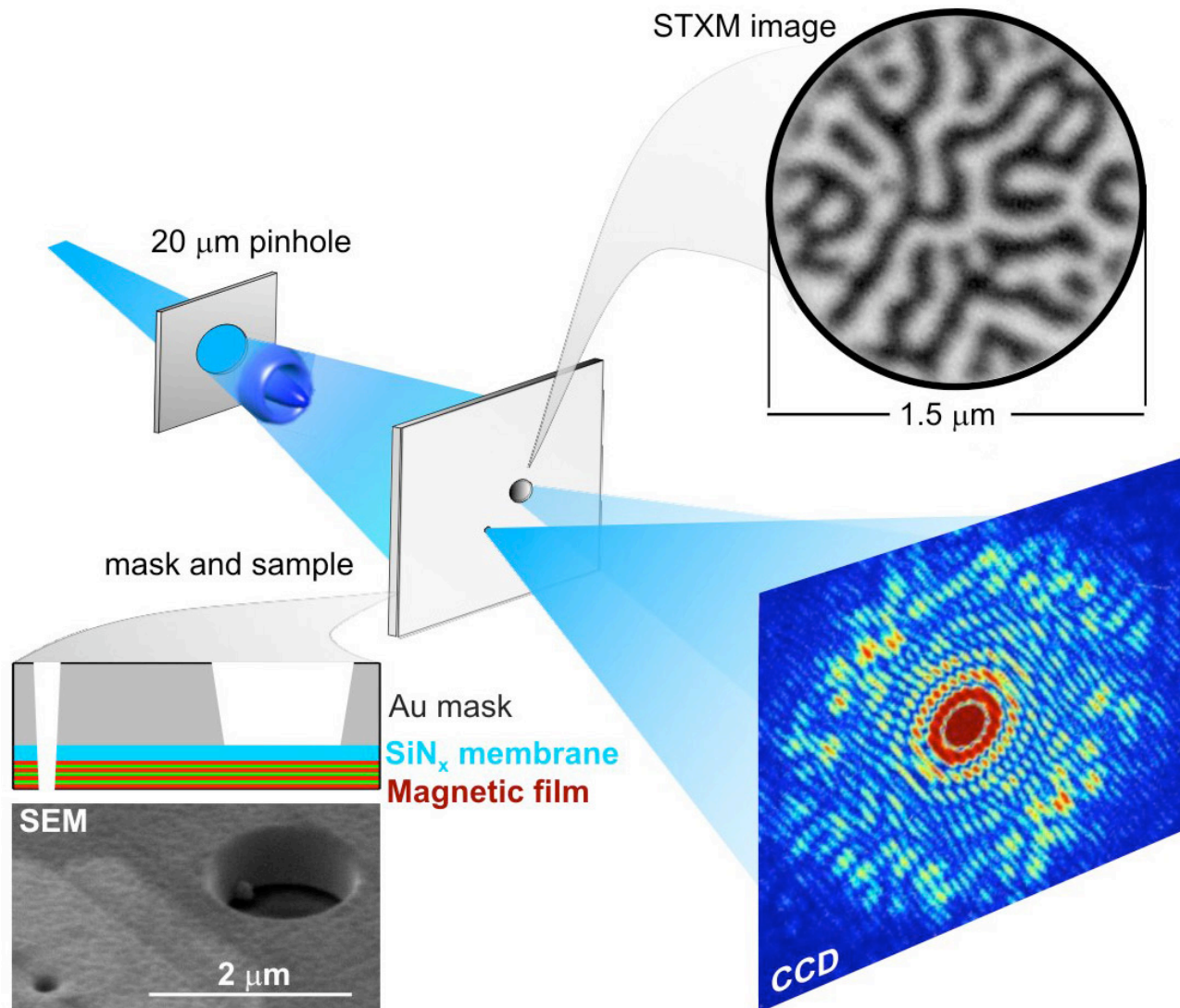
1.7 GeV, 200 mA  
 $\lambda_u = 49$  mm,  $N = 84$   
 $0 \leq K \leq 2.5$   
 $\sigma_x = 314$   $\mu\text{m}$ ,  $\sigma_x' = 18$   $\mu\text{r}$   
 $\sigma_y = 24$   $\mu\text{m}$ ,  $\sigma_y' = 2$   $\mu\text{r}$   
 $\eta_{\text{euv}} = 10\%$  ;  $\eta_{\text{sxr}} = 10\%$



Ch08\_BESSYII\_Nov07.ai



# Lensless imaging of magnetic nanostructures by x-ray spectro-holography



S. Eisebitt, J. Lüning, W.F. Schlotter, M. Lörger, O. Hellwig,  
W. Eberhardt & J. Stöhr / *Nature*, 16 Dec 2004

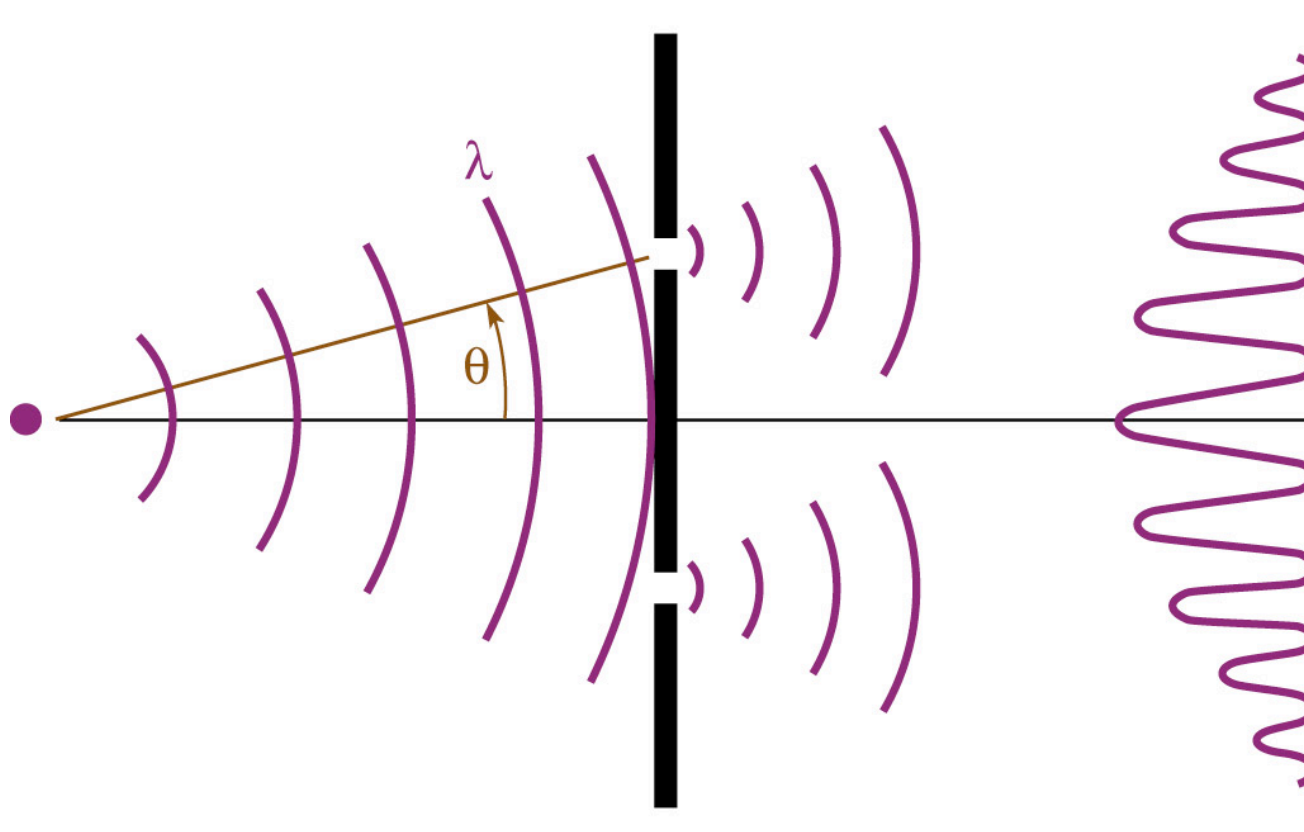
LenslessImagingF1.ai

CheironSchool\_Oct2010\_Lec2.ppt

# Undulators, FELs and coherence

- Spatial coherence
- Temporal coherence
- Partial coherence
- Full coherence
- Spatial filtering
- Uncorrelated emitters
- Correlated emitters
- True phase coherence and mode control
- Lasers, amplified spontaneous emission (ASE) and mode control
- Undulator radiation
- SASE FEL **100<sup>+</sup> fsec soft/hard x-rays**
- Seeded FEL **true phase coherent x-rays**
- High harmonic generation (HHG) **compact fsec/asec EUV**
- EUV lasers and laser seeded HHG
- Applications with uncorrelated emitters
- Applications with correlated emitters

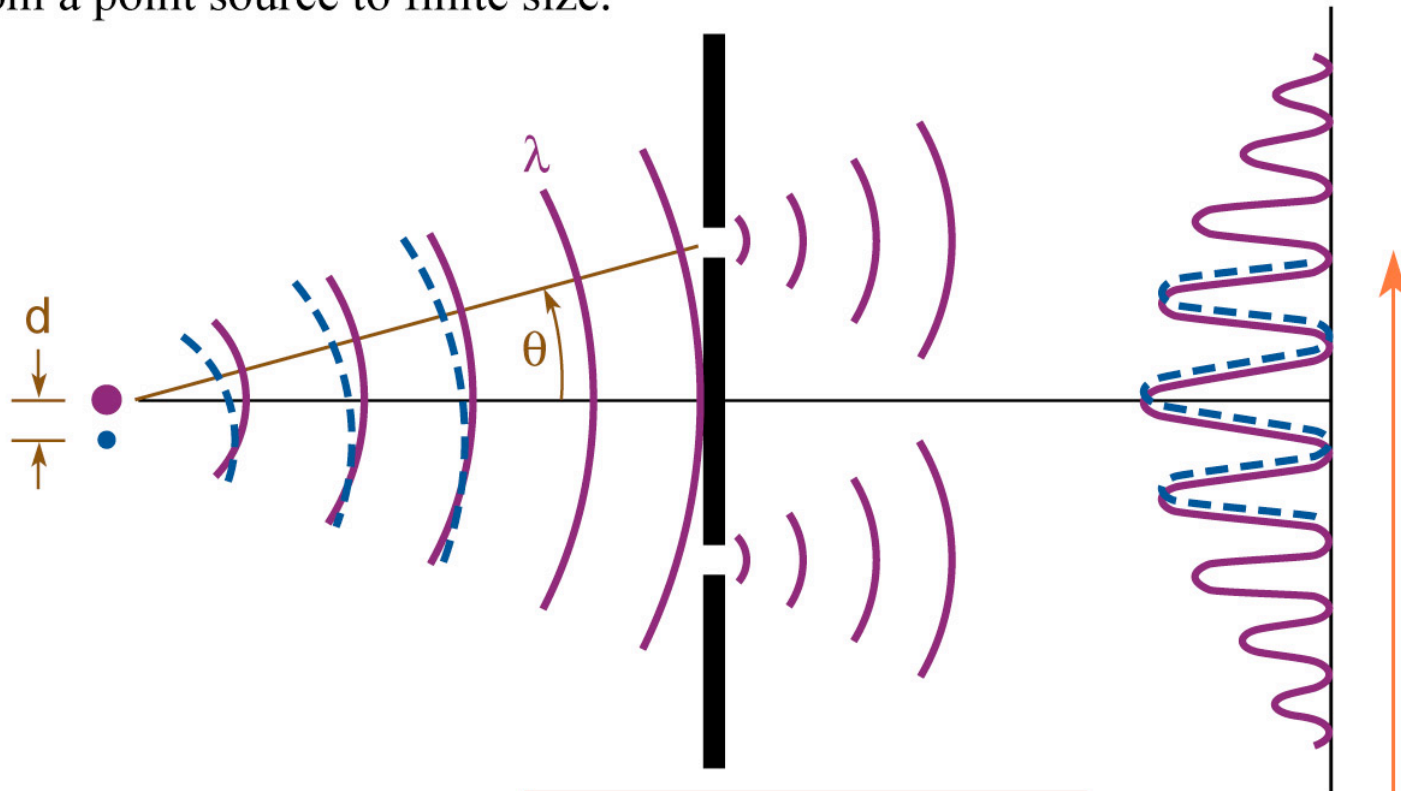
# Young's double slit experiment: spatial coherence and the persistence of fringes



YoungsExprmt.ai

# Young's double slit experiment: spatial coherence and the persistence of fringes

Persistence of fringes as the source grows from a point source to finite size.



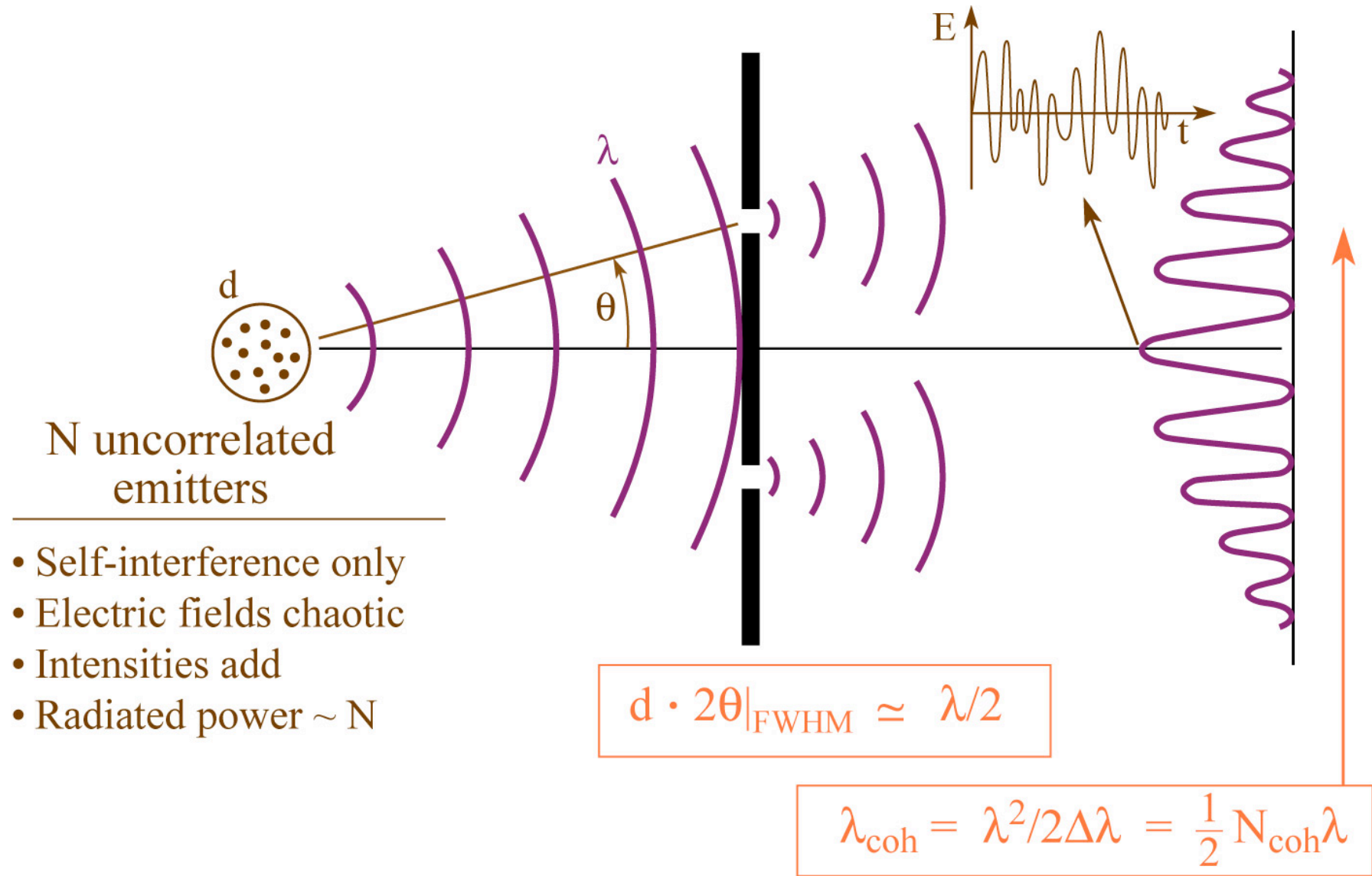
$$d \cdot 2\theta|_{\text{FWHM}} \approx \lambda/2$$

$$\lambda_{\text{coh}} = \lambda^2 / 2\Delta\lambda = \frac{1}{2} N_{\text{coh}} \lambda$$

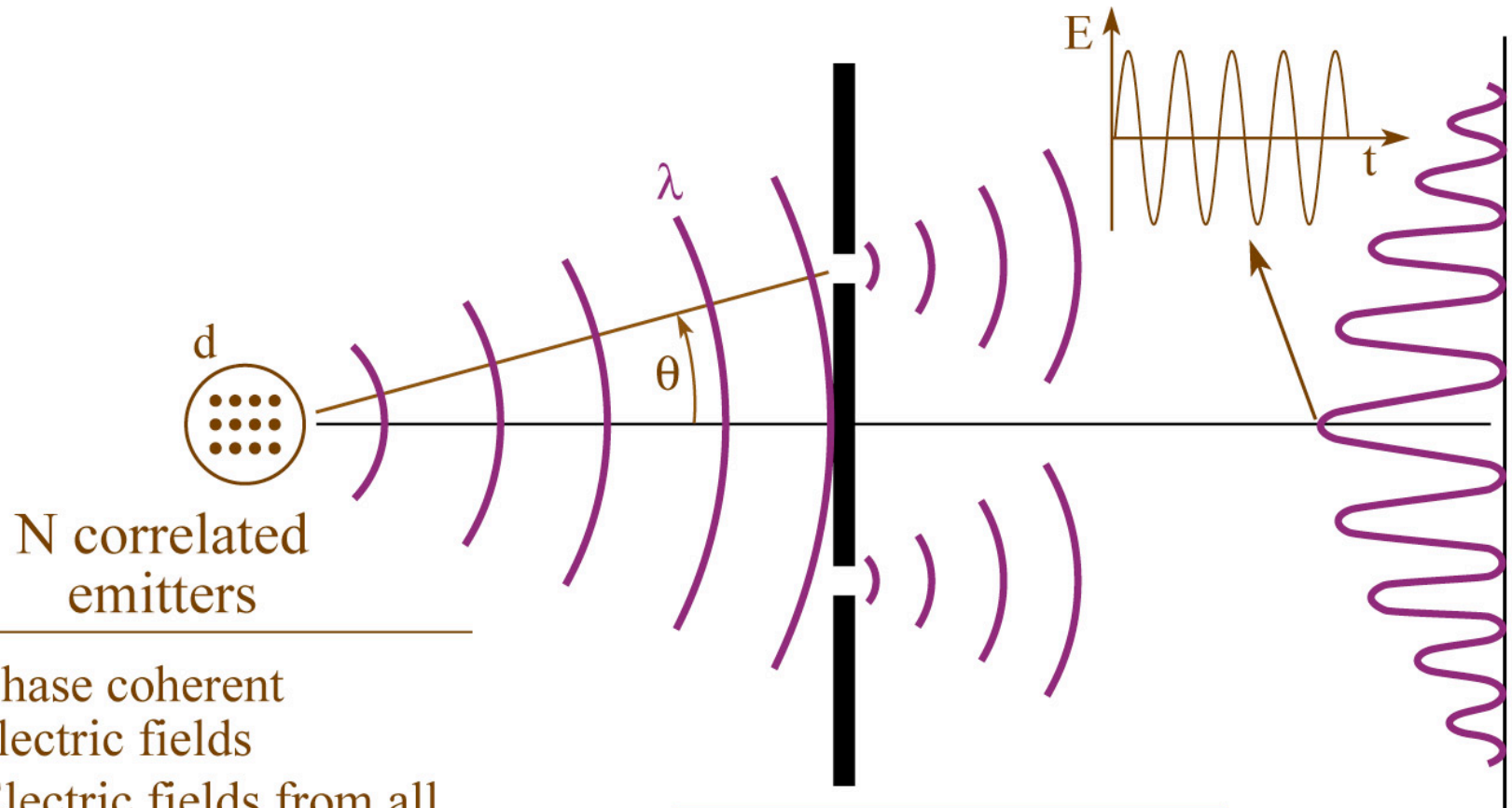
CH08\_YoungsExprmt\_v3.ai



# Young's double slit experiment with random emitters: Young did not have a laser



# Young's double slit experiment with phase coherent emitters (some lasers, or properly seeded FELs)



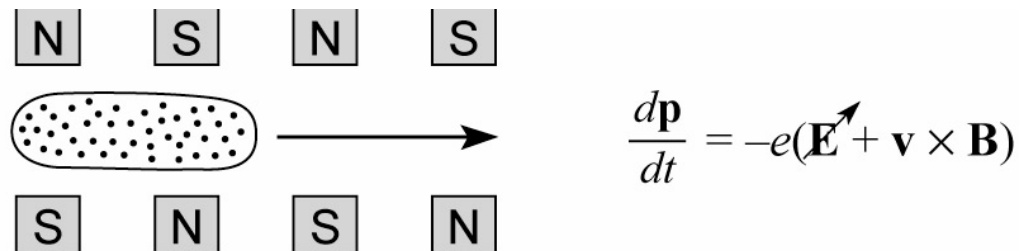
N correlated emitters

- Phase coherent electric fields
- Electric fields from all particles interfere constructively
- Radiated power  $\sim N^2$
- New phase sensitive probing of matter possible

$$d \cdot 2\theta_{\text{FWHM}} \approx \lambda/2$$

$$\lambda_{\text{coh}} = \lambda^2 / 2\Delta\lambda = \frac{1}{2} N_{\text{coh}} \lambda$$

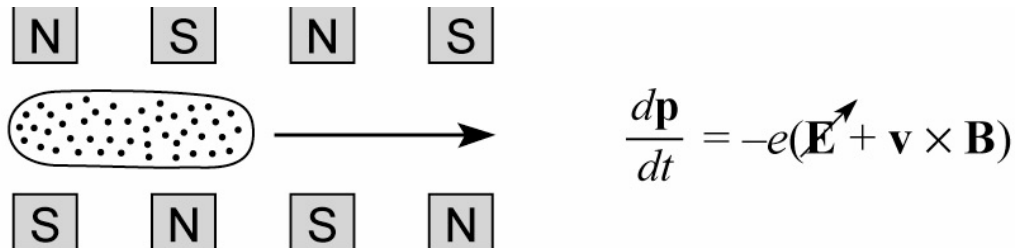
# Undulators and FELs



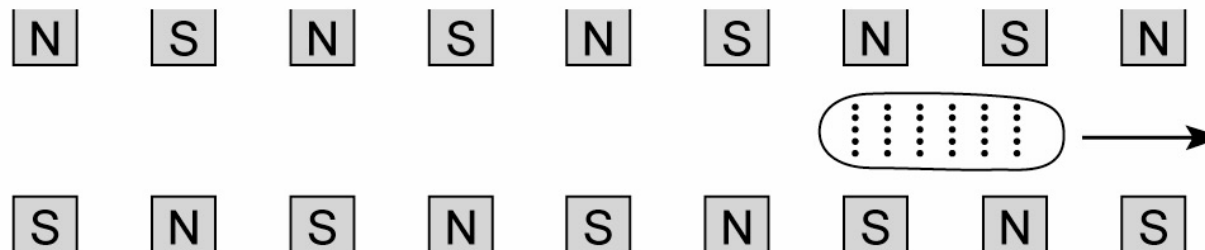
Undulator – uncorrelated electron positions, radiated fields uncorrelated, intensities add, limited coherence, power  $\sim N$ .

UndulatorsAndFELs1.ai

# Undulators and FELs



Undulator – uncorrelated electron positions, radiated fields uncorrelated, intensities add, limited coherence, power  $\sim N$ .

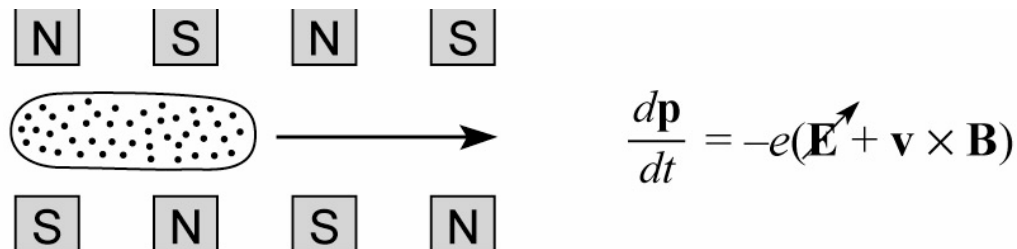


Free Electron Laser (FEL) – very long undulator, electrons are “microbunched” by their own radiated fields into strongly correlated waves of electrons, all radiated electric fields now add, spatially coherent, power  $\sim N^2$

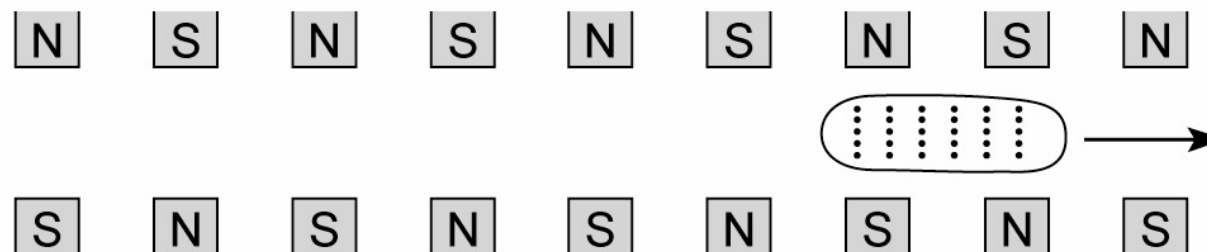
$$\frac{d\mathbf{p}}{dt} = -e(\mathbf{E} + \mathbf{v} \times \mathbf{B})$$



# Undulators and FELs



Undulator – uncorrelated electron positions, radiated fields uncorrelated, intensities add, limited coherence, power  $\sim N$ .

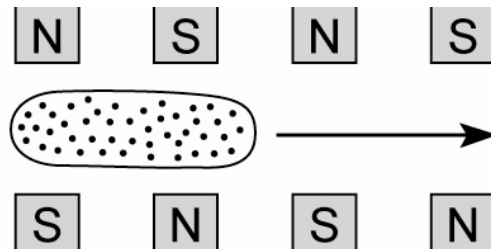


Free Electron Laser (FEL) – very long undulator, electrons are “microbunched” by their own radiated fields into strongly correlated waves of electrons, all radiated electric fields now add, spatially coherent, power  $\sim N^2$

$$\frac{d\mathbf{p}}{dt} = -e(\mathbf{E} + \mathbf{v} \times \mathbf{B})$$

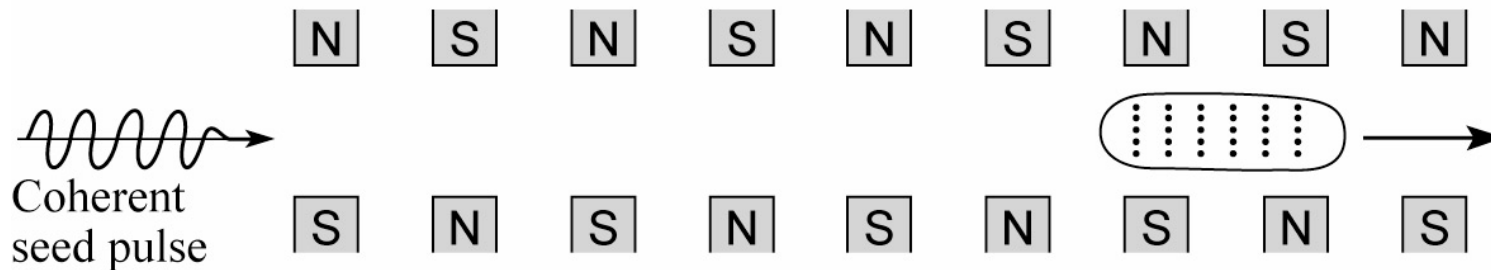
“SASE” FEL – no seed (several separate “waves” of electrons possible with uncorrelated phase.)  
Less peak power, broader spectrum.

# Seeded FEL



$$\frac{d\mathbf{p}}{dt} = -e(\mathbf{E} + \mathbf{v} \times \mathbf{B})$$

Undulator – uncorrelated electron positions, radiated fields uncorrelated, intensities add, limited coherence, power  $\sim N$ .

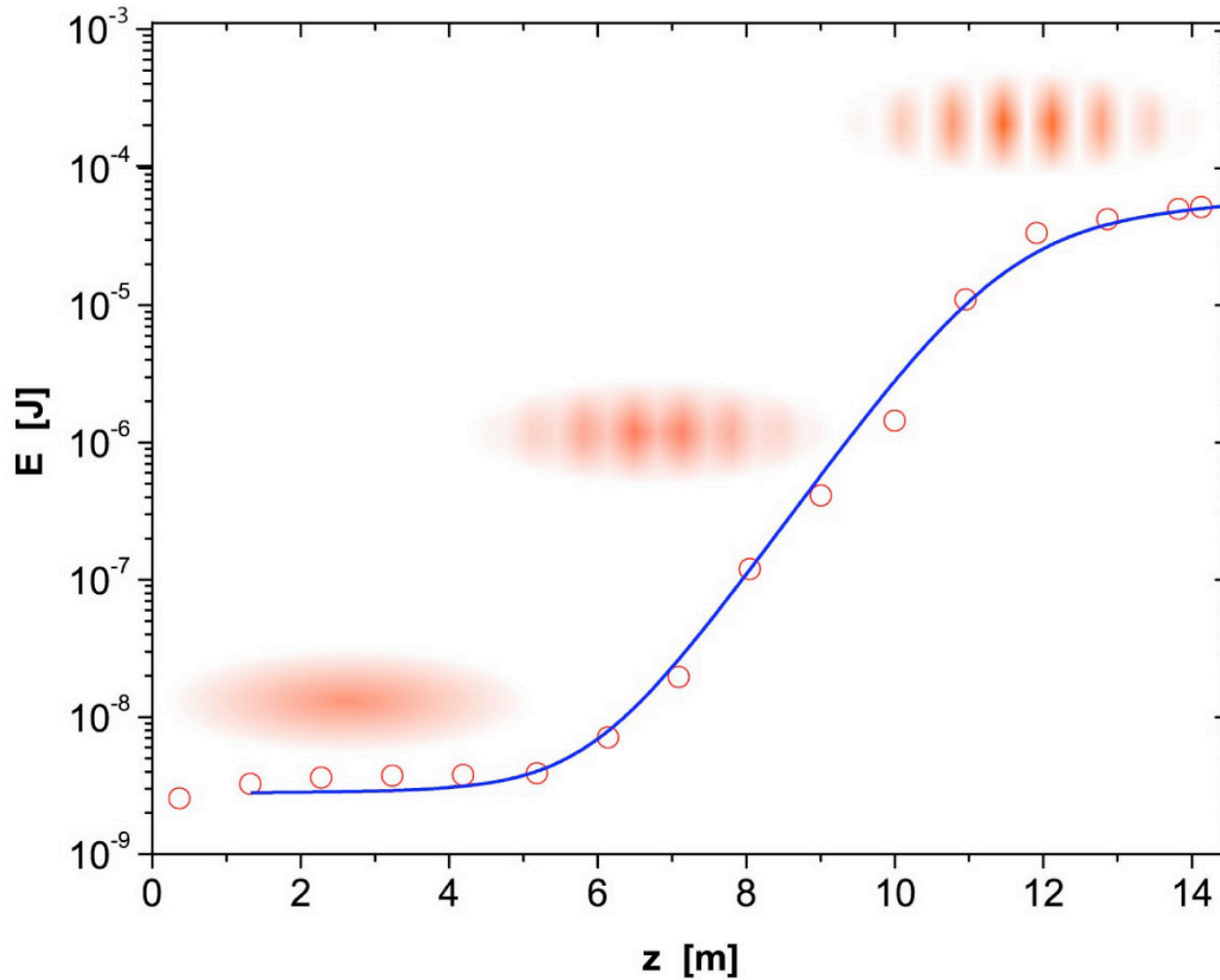


Free Electron Laser (FEL) – very long undulator, electrons are “microbunched” by their own radiated fields into strongly correlated waves of electrons, all radiated electric fields now add, spatially coherent, power  $\sim N^2$

$$\frac{d\mathbf{p}}{dt} = -e(\mathbf{E} + \mathbf{v} \times \mathbf{B})$$

Second generation x-ray FELs.

# Gain and saturation in an FEL



Courtesy of K-J. Kim

Gain\_Saturation\_FEL\_graph.ai

# Free Electron Lasers

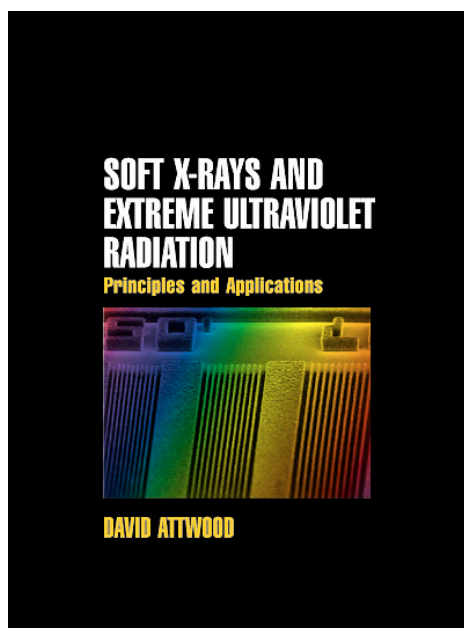
Parameters	Flash FEL (Hamburg)	LCLS (Stanford, 2010)	European XFEL (Hamburg, Schenefeld; 2014)
$E_e$	230/1000 MeV	13.6 GeV	17.5 GeV
$\gamma$	450/2000	26,600	35,000
$\lambda_u$	2.73 cm	3 cm	5 cm
$N$	500/1100	3700	4000
$L_u$	30 m	112 m	200 m
$\hbar\omega$	50-200 eV	0.8-10 keV	4-12 keV
$\lambda/\Delta\lambda$	100	350	1000
$e^-/\text{bunch}$	$10^9$	$6 \times 10^9$ (1 nC)	$6 \times 10^9$
$\Delta\tau$	25 fsec	160 fsec	100 fsec
$\dot{F}$	$3 \times 10^{12}$ ph/pulse	$2 \times 10^{12}$ ph/pulse	$10^{12} - 10^{14}$ ph/pulse
rep rate	1 Hz	120 Hz	10 Hz
$\hat{I}$	1.3 kA	3.4 kA	
$\hat{P}$	0.3 GW	8 GW	20-100 GW
$\hat{B}$	$1 \times 10^{28}$	$1 \times 10^{33}$	$5 \times 10^{33}$
$L$	260 m	5 km	3.4 km



## References

- 1) D. Attwood, *Soft X-Rays and Extreme Ultraviolet Radiation* (Cambridge, UK, 2000); available at Amazon.com.
- 2) J. Samson and D. Ederer, *Vacuum Ultraviolet Spectroscopy I and II* (Academic Press, San Diego, 1998). Paperback available.
- 3) J. Als-Nielsen and D. McMorrow, *Elements of Modern X-ray Physics* (Wiley, New York, 2001), 2nd edition (paperback).
- 4) A. Hofmann, *Synchrotron Radiation* (Cambridge, UK, 2004).

Ch05\_ReferencesSept2010.ai



Amazon.com



**UC Berkeley**

[www.coe.berkeley.edu/AST/sxreuv](http://www.coe.berkeley.edu/AST/sxreuv)

[www.coe.berkeley.edu/AST/srms](http://www.coe.berkeley.edu/AST/srms)

[www.coe.berkeley.edu/AST/sxr2009](http://www.coe.berkeley.edu/AST/sxr2009)